Research Square

Preprints are preliminary reports that have not undergone peer review.
They should not be considered conclusive, used to inform clinical practice,
or referenced by the media as validated information.

Tolerability and Clinical Benefit Assessment of Continuous Roginolisib Administration in Patients with Cancer including Metastatic Uveal Melanoma

Michele Maio

maio@unisi.it

University of Siena https://orcid.org/0000-0002-0323-6321

Anna Maria Di Giacomo

University of Siena, Italy, and Center for Immuno-Oncology, Department of Oncology, University Hospital of Siena

Matteo Simonelli

IRCCS Humanitas Research Hospital

Agnese Losurdo

Humanitas Clinical and Research Center

Pavlina Spiliopoulou

Beatson West of Scotland Cancer Centre https://orcid.org/0000-0002-6486-6319

Vincenzo D'Alonzo

University of Siena, University Hospital of Siena https://orcid.org/0000-0002-9264-377X

Giovanni Amato

University of Siena, University Hospital of Siena

Monica Valente

University of Siena, University Hospital of Siena

Hugo Barcenilla

Karolinska Institutet https://orcid.org/0000-0002-7255-362X

Anette Johnsson

Karolinska Institutet

Laura Gonzalez

Karolinska Institutet

Ziyang Tan

Karolinska Institutet

Lakshmi Kanth Tadepally

Karolinska Institutet https://orcid.org/0000-0001-7256-5770

Petter Brodin

Karolinska Institutet https://orcid.org/0000-0002-8103-0046

Michael Lahn
iOnctura SA
Giusy Di Conza
iOnctura SA https://orcid.org/0000-0003-1353-5867
Rebeca Zorrilla
iOnctura SA
Lars van der Veen
iOnctura SA
Alessio Bevilacqua
iOnctura https://orcid.org/0000-0001-7009-4362
Paramjit Kaur
iOnctura SA
Tracey Hammett
iOnctura SA
Marco Durini
Fortrea
Andrea Corsi
radiomics.bio https://orcid.org/0000-0003-3954-303X
Nikhil Sindhwani
Radiomics.bio
Mariaelena Occhipinti
San Cataldo Hospital
Robert Snijder
BOTh Analytics GmbH
Ayad Abdul-Ahad
BOTh Analytics GmbH
Aniko Meijer
BioLizard NV
Umberto Postiglione
BioLizard NV
Gregory Price
Indiana University Health Simon Cancer Center
Gillian Hopton
Veramed Ltd.
Emily Wood
Veramed Ltd.
Vincent Vuaroqueaux
4HF Biotec https://orcid.org/0000-0001-9120-5332
Anne-Lise Peille

4HF Biotec GmbH

Jill Graham

Beatson West of Scotland Cancer Centre, School of Cancer Sciences, University of Glasgow

Ming Poi

Caris Life Sciences https://orcid.org/0000-0001-6065-8662

David Spetzler

Caris Life Sciences https://orcid.org/0000-0002-9531-0970

Carmelo Carlo-Stella

Humanitas Research Center - IRCCS https://orcid.org/0000-0003-3144-0124

Armando Santoro

Humanitas Clinical and Research Center IRCCS, Humanitas Cancer Center https://orcid.org/0000-0003-1709-9492

Jeff Evans

Beatson

Article

Keywords:

Posted Date: December 17th, 2025

DOI: https://doi.org/10.21203/rs.3.rs-8048398/v1

License: This work is licensed under a Creative Commons Attribution 4.0 International License. Read Full License

Additional Declarations: Yes there is potential Competing Interest. I am an employees of the study Sponsor (iOnctura) with stock options.

Version of Record: A version of this preprint was published at Nature Communications on October 9th, 2026. See the published version at https://doi.org/10.1038/s41467-026-77358-7.

Abstract

Phosphatidylinositol 3-kinase delta (PI3Kδ) promotes tumour cell growth directly or indirectly by activating immune-suppressive cells. Roginolisib is a selective, non-ATP competitive inhibitor, which locks PI3Kδ into an inactive state. In a First-in-Human dose study, continuous daily dosing of roginolisib was investigated in patients with solid and haematologic malignancies. In Part A, 24 patients received escalating doses of roginolisib. In Part B, 20 mostly pre-treated metastatic uveal melanoma (mUM) patients received a dose associated with continuous PI3Kδ inhibition of > 90%. No Dose Limiting Toxicity or drug related toxicities requiring dose modifications were observed (≥ Grade 3 toxicities: 3/44; 6.8%). In mUM, median Overall Survival (mOS) was 20.8 months. mOS in mUM patients with Stable Disease was 28.5 months, and in patients with Progressive Disease was 12.3 months. Roginolisib treatment was associated with reducing T regulatory cell abundance, increasing activated $CD8^+$ T cells and soluble plasma IL-15.

Introduction

Phosphatidylinositol 3-kinase (PI3K) is a family of enzymes involved in cellular functions such as cell growth, proliferation, differentiation, motility, survival and intracellular trafficking[1,2]. A member of this family, phosphatidylinositol 3-kinase delta (PI3Kδ), is predominantly found in white blood cells[3]. In haematologic malignancies, PI3Kδ is associated with progression of B cell malignancies and blocking its tumour-cell intrinsic activity can reduce tumour cell proliferation[4]. In solid tumours, the tumour cell-intrinsic role is less well established, although PI3Kδ expression is found in highly transformed cells[5,6]. In addition to these tumour-cell intrinsic roles, PI3Kδ expression plays a role in the activation of T regulatory (Treg) cells[7]. PI3Kδ-dependent activation of immune suppressive Treg cells or myeloid-derived suppressor cells contributes to tumour cell extrinsic malignant growth [6]. Pro-inflammatory mediators, such as Tumour Necrosis Factor alpha, can activate PI3Kδ expression in fibroblasts and endothelial cells and further enhance the tumour cell growth via neo-angiogenesis[8]. Inhibiting this tumour cell extrinsic role of PI3Kδ pharmacologically has potent anti-tumour effects, especially in combination with immune checkpoint inhibitors (ICI)[9]. Based on the role of PI3Kδ in different cancers, PI3Kδ small molecule inhibitors were developed, initially targeting B cell malignancies[4]. Most of these first-generation inhibitors were designed to compete directly with intracellular adenosine triphosphate (ATP) for binding to the active form of the kinase[10]. Using such ATP-competitive inhibitors, high selectivity remained challenging based on the conserved nature of the ATP-binding pocket. Next-generation non-ATP competitive inhibitors may achieve improved selectivity by exploiting allosteric binding sites and/or regulatory features that are unique to the individual kinases, and maintain potency at high ATP concentrations[11]. Roginolisib is such a novel next-generation, selective and non-ATP competitive PI3Kδ inhibitor[12,13]. Similar to the first-generation PI3K inhibitors, roginolisib selectively reduces proliferation of Treg cells, while preserving $CD8^+$ T and $CD4^+$ T cell expansion[12]. Contrary to idelalisib, roginolisib does not promote differentiation of conventional $CD4^+$ T cells into T helper (Th) 1,

Th2, and Th17 subsets associated with immune toxicity (Solli et al, 2025. Manuscript submitted to Molecular Oncology). Roginolisib blocks tumour-cell intrinsic effects of PI3Kδ in lymphoma models, as well as models of solid tumours, such as mesothelioma[14], colorectal, pancreatic, and lung cancers[12]. In malignant B cells, including cells from chronic lymphocytic leukaemia patients resistant to Burton Tyrosine Kinase (BTK) inhibitors, roginolisib can block proliferation directly, either as monotherapy or in combination with other agents[12,15].

The First in Human (FiH) dose study of roginolisib was conducted in patients with predicted high PI3Kδ expression, including metastatic cutaneous and uveal melanoma (mCM and mUM), and follicular Non-Hodgkin lymphoma (NHL-FL). In such patients, the dose selection was based on a predictive pharmacokinetic (PK)/pharmacodynamic model derived from exposure and pharmacodynamic-effects, e.g., phosporlyated protein kinase B (pAKT) expression, in non-clinical models[13]. In-liu of measuring changes in expression of pAKT in blood or tumour cells, a standardised basophil activation test (BAT) was used to measure the PI3Kδ-associated pharmacodynamic effects in participants[16]. Using this approach, we determined 80 mg daily dose as a safe Biologically Effective Dose (BED), which can inhibit PI3Kδ at the calculated Inhibitory Concentration of 90% (IC90).

Results

Introduction to General Design

In the present FiH dose study, patients with cancer who had malignancies with high PI3Kδ expression or high Treg cell presence, according to The Cancer Genome Atlas (TCGA) databases, were enrolled to evaluate the benefit/risk of roginolisib (Supplement Fig. 1). Forty-four patients, including patients with mCM, mUM, NHL-FL, and mesothelioma, were enrolled from February 2020 to December 2024 (Table 1). The study consisted of a dose escalation part (Part A) to confirm the anticipated BED and a subsequent dose expansion (Part B) at the BED (Fig. 1a).

Table 1
Patient Demographics and Baseline Characteristics

	Uveal Melanoma	Cutaneous Melanoma	Mesothelioma	NHL-FL	Overall
	n (%)	n (%)	n (%)	n (%)	n (%)
Safety population	29	5	2	8	44
Efficacy population	27	4	1	8	40
Age (years)					
Median (range)	56.0 (27–82)	73.0 (44–76)	61.5 (51–72)	70.5 (55–75)	59.0 (27–82)
Sex					
Male	14 (48.3)	4 (80.0)	1 (50.0)	3 (37.5)	22 (50.0)
Female	15 (51.7)	1 (20.0)	1 (50.0)	5 (62.5)	22 (50.0)
ECOG (%)					
0	24 (82.8)	3 (60.0)	1 (50.0)	4 (50.0)	32 (72.7)
1	5 (17.2)	2 (40.0)	1 (50.0)	4 (50.0)	12 (27.3)
Time since initial diagnosis (months)					
n	29	5	2	8	44
Median (range)	75.8 (3-501)	46.5 (39–104)	38.8 (4–73)	69.1 (33–163)	71.1 (3-501)
Disease progressed on the last treatment					

ECOG stands for Eastern Cooperative Oncology Group, N stands for the total number of participants, n stands for number of participants, NA stands for not applicable, NHL-FL stands for Non-Hodgkin lymphoma - follicular lymphoma

[a]Entered Extension phase in which patients continued on treatment. Treatment was recorded as discontinued in the main study in order to move patients into the extension phase. [b]2 further patients received tebentafusp, 1 as adjuvant and 1 as third-line.

	Uveal Melanoma	Cutaneous Melanoma	Mesothelioma	NHL-FL	Overall
	n (%)	n (%)	n (%)	n (%)	n (%)
Yes	29 (100)	5 (100)	2 (100)	7 (87.5)	43 (97.7)
No	0	0	0	1 (12.5)	1 (2.3)
Current site of metastatic disease					
Bone	6 (20.7)	1 (20.0)	0	NA	7 (15.9)
Liver	26 (89.7)	2 (40.0)	0	NA	28 (63.6)
Lung	16 (55.2)	2 (40.0)	1 (50.0)	NA	19 (43.2)
Lymph node	7 (24.1)	4 (80.0)	0	NA	11 (25.0)
Skin or subcutaneous tissue	4 (13.8)	3 (60.0)	0	NA	7 (15.9)
BRAF mutation status					
Mutated	NA	3 (60.0)	NA	NA	3 (6.8)
Wild type	NA	2 (40.0)	NA	NA	2 (4.5)
Prior therapy for cancer treatment					
Yes	26 (89.7)	5 (100)	2 (100)	8 (100)	41 (93.2)
No	3 (10.3)	0	0	0	3 (6.8)
First-line					
Pembrolizumab	11 (37.9)	1 (20.0)	0	0	12 (27.3)

ECOG stands for Eastern Cooperative Oncology Group, N stands for the total number of participants, n stands for number of participants, NA stands for not applicable, NHL-FL stands for Non-Hodgkin lymphoma - follicular lymphoma

[a]Entered Extension phase in which patients continued on treatment. Treatment was recorded as discontinued in the main study in order to move patients into the extension phase. [b]2 further patients received tebentafusp, 1 as adjuvant and 1 as third-line.

	Uveal Melanoma	Cutaneous Melanoma	Mesothelioma	NHL-FL	Overall
	n (%)	n (%)	n (%)	n (%)	n (%)
Nivolumab	8 (27.6)	1 (20.0)	0	0	9 (20.5)
Bendamustine; rituximab	0	0	0	5 (62.5)	5 (11.4)
Ipilimumab; nivolumab	3 (10.3)	1 (20.0)	0	0	4 (9.1)
Cyclophosphamide; doxorubicin hydrochloride; prednisone; rituximab; vincristine sulphate	0	0	0	3 (37.5)	3 (6.8)
Ipilimumab	3 (10.3)	0	0	0	3 (6.8)
Rituximab	0	0	0	2 (25.0)	2 (4.5)
Second-line					
Ipilimumab	10 (34.5)	3 (60.0)	0	0	13 (29.5)
IMCgp 100[b]	2 (6.9)	0	0	0	2 (4.5)
Nivolumab	2 (6.9)	0	0	0	2 (4.5)
Total number of prior lines of therapy					
n	26	5	2	8	41
Median (range)	2.0 (1–7)	3.0 (2–5)	2.5 (1–4)	1.5 (1–8)	2.0 (1–8)
Primary reason for study discontinuation [a]					
Lost to follow-up	0	1 (20.0)	0	2 (25.0)	3 (6.8)
Death	14 (48.3)	3 (60.0)	2 (100)	1 (12.5)	20 (45.5)

ECOG stands for Eastern Cooperative Oncology Group, N stands for the total number of participants, n stands for number of participants, NA stands for not applicable, NHL-FL stands for Non-Hodgkin lymphoma - follicular lymphoma

[a]Entered Extension phase in which patients continued on treatment. Treatment was recorded as discontinued in the main study in order to move patients into the extension phase. [b]2 further patients received tebentafusp, 1 as adjuvant and 1 as third-line.

	Uveal Melanoma	Cutaneous Melanoma	Mesothelioma	NHL-FL	Overall
	n (%)	n (%)	n (%)	n (%)	n (%)
Entered extension study	15 (51.7)	1 (20.0)	0	5 (62.5)	21 (47.7)
Primary reason for treatment discontinuation					
Physician decision	0	0	0	1 (12.5)	1 (2.3)
Death	2 (6.9)	1 (20.0)	1 (50.0)	0	4 (9.1)
Progressive disease	18 (62.1)	2 (40.0)	1 (50.0)	7 (87.5)	28 (63.6)
Entered extension phase[a]	8 (27.6)	1 (20.0)	0	0	9 (20.5)
Other	1 (3.4)	1 (20.0)	0	0	2 (4.5)

ECOG stands for Eastern Cooperative Oncology Group, N stands for the total number of participants, n stands for number of participants, NA stands for not applicable, NHL-FL stands for Non-Hodgkin lymphoma - follicular lymphoma

[a]Entered Extension phase in which patients continued on treatment. Treatment was recorded as discontinued in the main study in order to move patients into the extension phase. [b]2 further patients received tebentafusp, 1 as adjuvant and 1 as third-line.

Baseline Characteristics and Demographics

Eligible patients had either progressed on their last standard therapy or had contra-indication to receive approved therapies (Table 1). The median age of patients was 59 years (range: 27–82) with an equal ratio of male and female patients. The majority of patients had Eastern Cooperative Oncology Group (ECOG) performance status (PS) of 0 (32/44; 72.7%).

Patients with mUM had the longest time since initial diagnosis and patients with mesothelioma the shortest (Table 1). Except for 3 mUM patients, all other mUM patients had at least one prior systemic therapy. The majority of mUM patients (N = 29) had liver (89.7%) and lung (55.2%) metastases. mUM patients had mostly an ECOG PS equal to 0 (24/29; 82.8%). Most mUM patients (17/29; 59%) had lactate dehydrogenase (LDH) levels above the upper limit of normal (ULN) at baseline (Supplement Table S2). Alkaline phosphatase (ALP) levels were elevated in 12 mUM patients (41%). Using the largest liver lesion, 55% (16/29) of mUM patients had stage pM1b (> 3 cm to ≤ 8 cm) and 28% (8/29) stage pM1c (> 8 cm)[17] (Supplement Table S2) disease. The most common 1st line treatment for mUM patients was pembrolizumab (11/29; 37.9%), followed by nivolumab (8/29; 27.6%) and ipilimumab (6/29; 20.7%). The most common 2nd line treatment was ipilimumab (10/29; 34.5%). Two patients (2/29; 6.9%) received

prior tebentafusp (IMCgp 100) as 2nd line treatment. Among the patients with mCM (N = 5), there were 3 patients who had *BRAF* mutations (3/5; 60%).

Tolerability

Roginolisib was administered as a daily morning dose and compliance across all cycles was over 97% across all doses. Overall median exposure was 144.5 days (4.7 mo; 0.5–37.3 mo). The median exposure for all 29 mUM patients was 171 days (5.6 mo; 1-35.9 mo) and for patients receiving 80 mg it was 221 days (7.3 mo; 1-22.1 mo). A Grade 2 roginolisib-related diarrhoea led to the reduction from 80 mg to 60 mg in one patient. Dose interruptions and omissions were reported for 23 patients, the majority unrelated to roginolisib, such as SARS-Cov2 infection or vaccination and palliative, disease-related interventions (Supplement Table S1). In Part A, four patients, initially treated at lower doses, had an intra-patient dose escalation to 80 mg after the 80 mg dose was declared safe (i.e., 1 patient escalated from 10 mg; 1 from 20 mg and 2 from 40 mg).

The overall high compliance was likely due to the favourable toxicity profile. No dose-limiting toxicities (DLTs) were observed or maximum tolerated dose (MTD) declared at any dose level (Table 2). Seven (15.9%) patients had 9 serious adverse events (SAEs), all considered unrelated to roginolisib. Three SAEs had an outcome of death, all of which were associated with progressive disease. The all-cause treatment-emergent adverse events (TEAEs) were 88.6% (39/44) for Grade 1 and 59.1% (26/44) for Grade 2 (Table 2). The drug-related TEAEs were 38.6% (17/44) for Grade 1 and 13.6% (6/44) for Grade 2. The rate of all-cause Grade ≥ 3 TEAEs was 25% (11/44) and for drug-related was 6.8% (3/44) (Table 2). One patient with mUM (1/44; 2.3%) experienced a life-threatening (Grade 4) TEAE of hyperbilirubinaemia unrelated to roginolisib and related to disease progression. The TEAEs were not associated with a specific organ group regardless of causality (Supplement Tables S3-S6). The majority of Grade 3 events were related to “laboratory investigations” and occurred in 6 patients (6/44; 13.6%), of which 3 (3/44; 6.8%) were deemed as treatment-related. These three Grade 3 AEs (i.e., platelet count decreased, lipase increased, neutrophil count decreased) were transient and resolved while receiving roginolisib. Among the UM patients only one patient discontinued roginolisib due to a Grade 2 uveitis, which emerged during the initial 28-day cycle. The patient had experienced similar symptoms on prior pembrolizumab treatment.

Table 2
Overall summary of treatment-emergent adverse events by indication

	Uveal melanoma	**Cutaneous melanoma**	**Mesothelioma**	**NHL-FL**	**Overall**
	(N = 29)	**(N = 5)**	**(N = 2)**	**(N = 8)**	**(N = 44)**
	n (%)	**n (%)**	**n (%)**	**n (%)**	**n (%)**
Any TEAEs	27 (93.1)	5 (100)	2 (100)	8 (100)	42 (95.5)
Any serious TEAEs	4 (13.8)	2 (40.0)	1 (50.0)	0	7 (15.9)
TEAEs related to roginolisib [a]	15 (51.7)	0	2 (100) 2	4 (50.0) 10	21 (47.7)
Serious TEAEs related to roginolisib [a]	0	0	0	0	0
TEAEs leading to death [b]	1 (3.4)	1 (20.0)	1 (50.0)	0 0	3 (6.8)
TEAEs leading to any drug interruption	19 (65.5)	2 (40.0)	0	2 (25.0)	23 (52.3)
TEAEs leading to discontinuation from study treatment	1 (3.4)	0	0	0	1 (2.3)
TEAEs ≥ Grade 3	10 (34.5)	1 (20.0)	1 (50.0)	2 (25.0)	14 (31.8)
TEAEs ≥ Grade 3 related to roginolisib	1 (3.4)	0	0	2 (25.0)	3 (6.8)
Immune-related TEAEs	1 (3.4)	0	0	0	1 (2.3)
Protocol-defined DLT and related to roginolisib [a]	0	0	0	0	0

AE stands for adverse event, DLT stands for dose-limiting toxicity, E stands for number of events, N stands for total number of participants, n stands for number of participants, NHL-FL stands for non-Hodgkin lymphoma, subtype follicular lymphoma, stands for TEAE = treatment-emergent adverse event.

[a] Cases with missing relationship of the AE to study drug were considered treatment-related

[b] Grade 5 AEs and/or AEs with the outcome “death” were considered as AEs leading to death

The denominator for percentages is the number of participants in the safety population for each group.

	Uveal melanoma	Cutaneous melanoma	Mesothelioma	NHL-FL	Overall
	(N = 29)	(N = 5)	(N = 2)	(N = 8)	(N = 44)
	n (%)	n (%)	n (%)	n (%)	n (%)
TEAEs by CTCAE Grade					
1	26 (89.7)	4 (80.0)	2 (100%)	7 (87.5)	39 (88.6)
2	19 (65.5)	3 (60.0)	2 (100)	2 (25.0)	26 (59.1)
3	8 (27.6)	0	0	2 (25.0)	10 (22.7)
4	1 (3.4)	0	0	0	1 (2.3)
TEAEs by CTCAE Grade related to roginolisib					
1	12 (41.4)	0	2 (100)	3 (37.5)	17 (38.6)
2	5 (17.2)	0	0	1 (12.5)	6 (13.6)
3	1 (3.4)	0	0	2 (25.0)	3 (6.8)
4	0	0	0	0	0
AE stands for adverse event, DLT stands for dose-limiting toxicity, E stands for number of events, N stands for total number of participants, n stands for number of participants, NHL-FL stands for non-Hodgkin lymphoma, subtype follicular lymphoma, stands for TEAE = treatment-emergent adverse event.					
[a] Cases with missing relationship of the AE to study drug were considered treatment-related					
[b] Grade 5 AEs and/or AEs with the outcome “death” were considered as AEs leading to death					
The denominator for percentages is the number of participants in the safety population for each group.					

Burden of Therapy (BoTH)

The safety profile of roginolisib was further investigated by using Burden of Therapy (BoTH) as part of an exploratory evaluation to detect changes in toxicity over time (Fig. 1b-c). The 80 mg continuous daily dosing showed no accumulation of toxicity when assessing the all-cause TEAEs (Fig. 1b) and was comparable to the toxicity profile of the lower doses of 10–40 mg once daily (Fig. 1c). Throughout the treatment the toxicity was predominantly mild or moderate (Supplement Fig. 2a-b).

PRO-CTCAE

Another measurement of toxicity was based on patient-reported outcomes using the PRO-CTCAE questionnaire. Among the 20 mUM patients enrolled in Part B, 16 patients completed 2 or more PRO-CTCAE assessments (16/20; 80%). Of the 157 expected assessments 139 were returned by patients (i.e., completion rate of 88.5%). At baseline, the patient-reported symptom burden was consistent with disease state. Overall, there was no worsening of symptoms over time, including the frequency of diarrhoea, abdominal pain or general pain (Fig. 1d, Supplement Fig. 2c-d). Improvements were observed in fatigue, abdominal pain and pain interference domains by Week 16 (= Cycle 5) for most patients (Fig. 1e-f, Supplement Fig. 2e). In later cycles, symptom worsening was reported coinciding with disease progression.

Pharmacokinetics

In addition to these safety evaluations, it was important to confirm that the daily continuous dosing achieved the predicted pharmacokinetic (PK) profile associated with selectively blocking PI3Kδ[18]. Roginolisib demonstrated a dose proportional PK profile with low to moderate variability. As predicted, roginolisib was rapidly absorbed with median t_{max} of approximately 1–2 hours post dose across all dose levels (Table 3). Exposure (AUC_{0-24} and C_{max}) on Cycle 1, Day 1 increased approximately proportionally over the dose range of 20 mg to 80 mg (80 mg: AUC_{0-24h} of 64000 ng*h/mL and C_{max} 4500 ng/mL and C_{min} 2130 ng/mL). A 4-fold increase in dose, resulted in a 3.29- and 3.58-fold increase in mean peak (C_{max}) and extent (AUC_{0-24}) of exposure increased, respectively. The half-life was approximately 24 hrs at the 80 mg dose. In Part B, the median steady-state trough concentration at Cycle 2, Day 1 was 1980 ng/mL (data not shown). The exposure at 20 or 80 mg was comparable in patients with solid malignancies and NHL-FL. Using high-sensitivity liquid chromatography-mass spectrometry (LC-MS/MS), plasma metabolites were detected with no relevant inter-subject variability following single and repeat oral administration of roginolisib. Each metabolite component represented less than 6% of the entire metabolite profile and no reactive metabolites were detected (unpublished data).

Table 3
Study IOA-244-101 Part A: Geometric Mean (%CV) PK Parameters of Roginolisib Following Single Oral Dose Administration of IOA-244 (ST and NHL-FL combined) (Cycle 1, Day 1)

Parameter (Units)	**Dose**			
	10 mg	**20 mg**	**40 mg**	**80 mg**
Patients, n	4	8	4	8
AUC_{0-24} (ng.h/mL)	14,300 (13.4) [d]	17,900 (34.4)	35,600 (11.4.)	64,000 (48.2)
AUC_{0-t} (ng.h/mL)	12,000 (32.0) [c]	17,800 (34.2)	35,800 (13.7) [c]	69,900 (43.6) [e]
$AUC_{0-\infty}$ (ng.h/mL)	37,800 (46.9) [d]	31,900 (47.7) [e]	88,800 (72.6) [c]	135,000 (128.5) [e]
C_{max} (ng/mL)	771 (21.9)	1,370 (31.7)	2,280 (30.8)	4,500 (26.2)
C_{min} [b] (ng/mL)	383 (36.8) [c]	512 (45.6)	1.210 (15.2) [c]	2,130 (59.7) [e]
t_{max} [a] (h)	1.50 (0.98-2.00)	1.00 (1.00–2.00)	2.04 (1.00–3.97)	1.00 (0.92–3.58)
$t_{1/2}$ (h)	34.7 (42.2) [d]	20.5 (21.3) [e]	29.4 (121.1) [c]	24.6 (110.7) [e]
CL/F (L/h)	0.264 (46.9) [d]	0.627 (47.7) [e]	0.450 (72.6) [c]	0.592 (128.5) [e]
V_z/F (L)	13.2 (3.9) [d]	18.5 (32.6) [e]	19.1 (36.2) [c]	21.0 (28.6) [e]

AUC stands for area under the curve, C_{max} stands for maximum observed plasma concentration, CL/F stands for apparent oral plasma clearance, n stands for number of participants, ST stands for solid tumour, NHL-FL stands for non-Hodgkin lymphoma, subtype follicular lymphoma, PK stands for pharmacokinetics, V/F stands for apparent volume of distribution during the terminal phase

[a] Median (min-max) presented; [b] Observed pre-dose concentration on Cycle 1, Day 2; [c] n = 3; [d] n = 2; [e] n = 7

Pharmacodynamics

The PK profile of roginolisib was correlated with results from the BAT assay, performed as previously described[16,19]. The dose-dependent pharmacodynamic effect of roginolisib had a variability of approximately 40%, and inhibition of CD63 expression plateaued at the 80 mg dose (Supplement Fig. 3a-d). At the 80 mg dose, steady-state trough concentrations of approximately 1940 ng/mL were above the PI3Kδ IC90 in human whole blood[12].

Anti-tumour responses and clinical benefit

Radiographic response assessments (e.g., RECIST 1.1) and time to event observations were used to document anti-tumour effects. For patients with solid malignancies, two patients had a partial response (PR) (2/32; 6.3%) (Table 4 and Fig. 2a). One PR was observed in a patient with mCM receiving the initial

20 mg dose, who progressed after 9.2 months. The patient's dose was increased to 80 mg and the disease stabilised. Currently, this patient remains on treatment with at least 60 months of daily dosing (Supplement Fig. 4a-b). The second PR was observed in a patient with mUM who received 80 mg (Fig. 2a). For patients with NHL-FL, time on treatment was longer at the 80 mg than at 20 mg (Supplement Fig. 4c). At the 80 mg dose, 1 of the 4 (1/4; 25%) patients with NHL-FL had a confirmed PR per Lugano criteria (Fig. 2b, Supplement Fig. 4d). Two additional patients (2/4; 50%) had a transient radiographic and clinical response, respectively. Clinical benefit also applied to patients with SD or long treatment periods and was based on 27 mUM patients who met the criteria for efficacy evaluation. For example, treatment for more than 6 months was observed in 55% (20/36) of patients with solid tumours, and in 33% (9/27) of mUM patients (Fig. 2c). The median (range) duration of clinical benefit in mUM patients was 7.4 months (95% CI: 3.7–16.5). At Week 16, two different mUM populations were observed, one with Stable disease (SD) and the other with Progressive Disease (PD) (Fig. 2d). At Week 16, 13 patients achieved SD (13/27; 48%); nine (9/27; 33%) patients had PD, and four (4/27; 15%) patients were censored. One patient achieved PR (1/27; 3.7%) (Supplemental Fig. 5f).

Table 4
Summary of Best Overall Response by Indication and in Patients Meeting Criteria for Efficacy Evaluation (Efficacy population)

	Solid tumour [a]				**NHL-FL [b]**		
	Metastatic Uveal melanoma	**Metastatic Cutaneous melanoma**	**Mesothelioma**	**Solid tumour overall**	**NHL-FL Cohort 1**	**NHL-FL Cohort 2**	**NHL-FL overall**
	(N = 27) n (%)	**(N = 4) n (%)**	**(N = 1) n (%)**	**(N = 32) n (%)**	**(N = 4) n (%)**	**(N = 4) n (%)**	**(N = 8) n (%)**
Best overall response							
CR	0	0	0	0	0	0	0
PR	1 (3.7)	1 (25.0)	0	2 (6.3)	0	1 (25.0)	1 (12.5)
SD	20 (74.1)	1 (25.0)	0	21 (65.6)	0	1 (25.0)	1 (12.5)
Progressive disease	6 (22.2)	2 (50.0)	1 (100)	9 (28.1)	4 (100)	2 (50.0)	6 (75.0)
Not evaluable	0	0	0	0	0	0	0
DCR at Week 16 (CR, PR or SD as OR) [c]	13 (48.1)	1 (25.0)	0	14 (43.8)	0	1 (25.0)	1 (12.5)

	Solid tumour [a]				NHL-FL [b]		
	Metastatic Uveal melanoma	Metastatic Cutaneous melanoma	Mesothelioma	Solid tumour overall	NHL-FL Cohort 1	NHL-FL Cohort 2	NHL-FL overall
	(N = 27) n (%)	(N = 4) n (%)	(N = 1) n (%)	(N = 32) n (%)	(N = 4) n (%)	(N = 4) n (%)	(N = 8) n (%)
BOR stands for best overall response, CR stands for complete response, DCR stands for disease control rate, N stands for total number of participants, n stands for number of participants, NHL-FL stands for non-Hodgkin lymphoma, subtype follicular lymphoma, OR stands for overall response, PR stands for partial response, RECIST stands for Response Evaluation Criteria in Solid Tumours, SD stands for stable disease.							
[a] Best overall response in target lesion was measured according to RECIST v1.1 for participants with solid tumours							
[b] Best overall response in sum of the products of the greatest perpendicular diameters was measured via the Lugano 2014 criteria for participants with NHL-FL							
[c] Week 16 overall response was taken from the Cycle 5 Day 1 assessment							
NHL-FL Cohort 1: roginolisib 20 mg; NHL-FL Cohort 2: roginolisib 80 mg.							
The denominator for percentages is the number of participants in the efficacy population for each group.							
Overall response rate: responders were participants with BOR of CR or PR; non-responders were all other participants.							

The overall median PFS was 3.8 months (95% CI: 3.6–5.8) for all patients with solid malignancies (n = 32), and 5.3 months (95% CI: 3.7–5.9) for mUM patients (n = 27) (Supplement Fig. 5a, Supplement Table S7). The 8 NHL-FL patients had a median PFS of 1.7 months (95% CI: 1.5–3.6) (Supplement Fig. 5b, Supplement Table S7).

Overall Survival (OS) was evaluated in 40 of 44 (90.9%) patients. For these 40 patients the median OS (mOS) was 28.5 months (95% CI: 11.3–31.8) (data cut off Dec-2023). Patients with mesothelioma had the shortest OS (Supplement Table S7). No differences in mOS were observed between the Part A and Part B for mUM patients. In mUM patients the mOS was 20.8 months (95% CI: 10.7–29.5), the mOS of patients with SD at Week 16 was 28.5 months (95% CI 14.2-NE), and the mOS for patients with PD at Week 16 was 12.3 months (95% 6.9-NE) (Fig. 2e, Supplement Table S7).

Given the encouraging observation in OS, complementary and exploratory studies were conducted to further characterise the activity of roginolisib. These studies included image analyses using radiomic methodologies, genomic studies in tumour tissue and cell-free DNA (cfDNA) to detect underlying genetic

drivers (e.g., driver mutations, HLA types), circulating immune cell analyses in blood by mass cytometry, plasma proteomics and tumour transcriptomics to assess molecular-based responses to roginolisib treatment. Immunohistochemistry (IHC) was used to study effects on the tumour immune infiltrate.

Exploratory imaging studies (mUM patients)

Volumetric changes of all evaluable metastatic lesions were assessed using computer tomography (CT) scans. A median of 31 lesions (range 2-281; Standard Deviation [SD]: 84.3) were present at screening with highest number of metastases in liver and lung. At screening, 23 patients had metastases in the liver, with a total of 326 lesions (median of 7; range: 1-135; SD: 27.3) and 13 patients had pulmonary metastases with 317 lesions (median of 8; range: 1-184; SD: 49.8). Tracking lesions in serial scans revealed mixed responses with several pre-existing tumour lesions disappearing or reducing while new lesions appeared or pre-existing lesions increased in volume (Fig. 2f). Interestingly, slower changes in tumour volume were observed in patients with SD at Week 16 based on RECIST 1.1 (Supplement Fig. 5c). Similar to first-generation PI3Kδ inhibitor, such as idelalisib 22, we also observed a reduction in spleen volume (Supplement Fig. 5d). In addition to the volumetric changes, we identified radiomic features for responding versus progressive lesions in liver metastases. In the 23 patients with baseline liver metastases, 59 lesions progressed and 127 responded by 24 weeks. Mixed effects modelling revealed that 63 radiomic features changed significantly over time, 59 features differed significantly between responding and non-responding lesions, and 84 features showed significantly different temporal trajectories (corrected p = 0.000467). After removing interfering factors, we found 17 unique informative features, including the quartile coefficient of dispersion (QCOD), a measure that quantifies the variability of voxel intensity within lesions (Supplement Fig. 5e)[20]. Similar features of intensity dispersion have been shown to correlate with immune system activity, p53 pathways, and cell cycle regulation in cancerous lesions, with prognostic significance for overall survival[21]. Non-responding lesions showed lower values of QCOD, indicating these lesions may exhibit higher textural homogeneity than responding lesions.

Genetic analysis (mUM patients)

To characterise the tumour genomic profile, whole exome sequencing (WES) was performed using DNA extracted from tumour tissue in 12 mUM patients (12/29; 41%) at baseline and after 5 weeks of treatment. In 62% of mUM patients (18/29) we also obtained cfDNA and evaluated the tumour DNA using the Caris Assure assay. Of the 12 patients with tumour tissue DNA, 6 patients (6/12; 50%) had also their cfDNA evaluated (Supplement Table S10 and S11). Among these 6 patients, tumour and cfDNA had similar mutations of *GNAQ*, *GNA11* and *BAP1* (5/6; 83%), while other mutations (e.g., *SMAD4*, *CHEK1*, *TP53*) were independently detected in either tumour tissue DNA or cfDNA (Supplement Fig. 6c, Supplement Table S11). In tumour tissue, gene alterations in *GNAQ*, *GNA11*, *BAP1*, and *SF3B1* were detected (Fig. 2g, Supplement Table S10). *GNAQ* and *GNA11* mutations were present both in patients with SD and PD at Week 16. All 5 patients with SD at Week 16 had a GNA11 mutation, while 4 of 7 patients with PD at Week 16 had a *GNAQ* mutation. Furthermore, in 17 mUM patients we found

HLA*02:01 in 3 patients (3/17; 18%), who had PD at Week 16 (Supplemental Table S13). Independently from tumour tissue DNA, exon variants of 13 pre-defined genes were evaluated in cfDNA samples from 18 mUM patients (Table S12). The average variant allele frequency (VAF) was calculated based on the presence of gene alterations (Supplement Table S10 and S12). VAFs changed mostly in patients with PD at Week 16, while patients with SD at Week 16 had few increases and no reductions (Supplement Fig. 6a, b).

Mass cytometry of circulating blood cells (mUM patients)

PI3Kδ inhibition is expected to elicit both phenotypic and quantitative alterations of immune cell populations, such as Tregs. Mass cytometry was performed on baseline and on treatment blood samples from 22 mUM patients. Most mUM patients had a decrease in $CD25^{+}/CD127^{low}$ Tregs over time (Fig. 3a). The population of $CD8^{+}CD39^{+}$ T cells, which reportedly increases in patients responding to ICI[22], increased over time (Fig. 3b). Conversely, $CD8^{+}CD39^{-}$ T cells and $CD56^{+}CD16^{-}$ NK cells decreased, (Fig. 3c and d, respectively). These reductions were more pronounced in patients with SD at Week 16 (Fig. 3a-d). The increase in $CD8^{+}CD39^{+}$ T cell frequency observed at Cycles 3 and 5 was positively correlated with OS (Fig. 3e, f). In contrast to these subsets, total $CD4^{+}$, $CD8^{+}$ T cell counts, $CD20^{+}$ B cell counts and immunoglobulin levels remained unchanged (Supplement Fig. 8a, b, c, e), apart from the total $CD14^{+}$ monocyte population which decreased during treatment.

Plasma proteomics (mUM patients)

To explore whether plasma proteins changes during treatment mirrored the immune cell changes, proteomic analysis was performed on samples from 23 mUM patients starting at baseline and at each cycle. Longitudinal assessment of proteins using the Olink technology identified significant changes in 83 of the 3,072 proteins (Fig. 4a). Some of these proteins are involved in B and T cell biology and were changed by treatments with first-generation PI3Kδ inhibitors, e.g., CXCL13 (previously known as B lymphocyte chemoattractant), CD160, FCRL2 (Fc receptor-like protein 2), CD5, CD5L, and CCL22 (Fig. 4b)[23]. Levels of CCL22, a chemokine known to recruit Treg cells[24], showed a positive correlation with Treg cell counts (Fig. 4d). Roginolisib treatment was also associated with increases in cytokines IL-15, IL-17D and soluble IFNGR2, while soluble PD1 was decreased (Fig. 4c). Interestingly, we also observed a reduction in CD5 and CD5L in plasma (Fig. 4b), which corresponded to a reduction in $CD5^{+}$ B cells (Fig. 4e). During treatment and focusing on patients with PD at Week 16, 208 plasma proteins changed, and among these 197 proteins increased (Fig. 4f, g). Among the 20 proteins with the highest increase, there were some, such as FKBP4 and AKT1S1, associated with the PI3K-mTOR pathway. FKBP4 fold change at Cycle 2 was negatively associated with OS (Supplement Fig. 9d). Other proteins connected to the PI3K-mTOR pathway, such as INPP5D (Src homology 2 domain containing inositol polyphosphate 5-phosphatase 1 SHIP1), PIK3AP1 (phosphoinositide-3-kinase adaptor protein 1), MYCBP2 (myc-binding protein 2), PFKFB2 (6-phosphofructo-2-kinase/fructose-2,6-biphosphatase 2), showed similar trends of increases over time in patients with PD at Week 16. By contrast, the same proteins showed a decreasing trend in patients with SD at Week 16 (Supplement Fig. 9a, b). In contrast

to patients with PD at Week 16, patients with SD at Week 16 had elevated PI3K-associated proteins at baseline (Supplement Fig. 9c).

Tumour transcriptomics (mUM patients) and IHC (Part A patients)

Biopsies offer insights to changes in the tumour and its microenvironment. In Part A, tumour biopsies were evaluated at baseline and after at least 4 weeks of treatment. Paired biopsies were obtained from 9/16 (56%) patients (either mCM or mUM patients), which showed a reduction in $Foxp3^+$ Treg cells in 6/9 pts (67%) (Fig. 5a), unchanged $CD8^+$ T cells (Fig. 5b) and consequently an increased $CD8^+$/Treg ratio (Fig. 5c).

In Part B, whole transcriptome sequencing of tumour biopsies (n = 14) was performed in mUM patients. In patients with SD at Week 16 (n = 7), 326 genes were significantly modulated (Fig. 5d), of which 325 genes were down- and one gene upregulated. The one upregulated gene was alpha-2-macroglobulin (A2M), which is expressed in normal uveal melanocytes and downregulated in uveal melanoma cells[25]. Using gene Ontology (GO) pathways enrichment analysis on all differentially regulated genes identified that pathways related to G-protein coupled receptors (GPCRs) were down-regulated, in particular those associated with olfactory receptors. (Fig. 5e, Supplement Fig. 9e).

Discussion

PI3Kδ plays a key role in the malignant process of solid and haematologic malignancies[1,2,26]. Although first-generation PI3Kδ inhibitors were effective in treating B cell malignancies, ATP-competitive inhibition was not able to establish a safety profile at an optimal dose, which eventually led to their withdrawal for most indications[26–28]. The toxicity profile of the first-generation PI3Kδ inhibitors was particularly challenging in patients with solid tumours[29–31].

Given this background, the objective of the FiH study was to define a safe dose for continuous daily dosing of roginolisib in both solid and haematologic malignancies. Contrary to a B cell specific target such as BTK, PI3Kδ can be expressed in several solid tumour cells (see TCGA and cell line data in Supplement Fig. 1a-b). To investigate roginolisib in PI3Kδ-enriched malignancies, we first verified that roginolisib administration achieved steady state plasma concentrations above the PI3Kδ IC90 in whole blood. Such concentrations were found to inhibit PI3Kδ-dependent signalling as measured by reduction in expression of the activation marker CD63 on basophils. The BAT assay confirmed consistent PI3Kδ inhibiton at the 80 mg dose, supporting PK/pharmacodynamic-guided dose selection.This approach parallels that used for first-generation PI3Kδ inhibitors, such as zandelisib[16]. In our study, BAT was used in patients with cancer for the first time at different doses and at monthly assessments, which may explain the larger variability observed in contrast to single-dose studies in healthy volunteers. In a subsequent roginolisib study in healthy volunteers, BAT was less variable and confirmed the 80 mg daily dose as the desired BED (manuscript in preparation). Once we demonstrated that the

PK/pharmacodynamic profile was consistent with the targeted PI3Kδ inhibition of ≥ 90%, we documented the tolerability and anti-tumour effects of roginolisib in patients.

During this FiH dose study, patients did not require dose modification, including patients with treatment duration of longer than 6 months. There were no serious infections or severe immune related adverse events, which were a concern for the first-generation PI3Kδ inhibitors, and no anti-infective prophylaxis was needed[29–31]. In fact, four patients who were on lower doses of roginolisib increased their dose to 80 mg without additional toxicities. At the 80 mg dose the majority of TEAEs related to roginolisib were Grade 1 and 2. While immune dysfunction was a key concern with first-generation PI3Kδ inhibitors, the total monthly CD4, CD8, NK and B lymphocyte populations were stable. Plasma immunoglobulin concentrations were also unchanged over time (Supplement Fig. 8e). This stable immune status may explain the low incidence of infection-related AEs (among which also infections with SARS-Cov-2). The weekly BoTh assessment, which reports weekly changes of AEs, also showed no additional toxicities at the 80 mg dose. Furthermore, the results of the PRO-CTCAE questionnaire suggested that roginolisib had a favorable toxicity profile, including a trend of improving fatigue in patients. While most first-generation PI3Kδ inhibitors report significant hepatic toxicities[32], these types of toxicities were not observed for roginolisib. As mUM patients have extensive liver metastases[33], liver-associated toxicities were closely monitored and no worsening of pre-existing liver or gastro-intestinal symptoms were observed. In most patients with pre-existing elevated liver enzymes, enzymes improved while patients received roginolisib without interruption.

Roginolisib´s safety profile may be the result of at least three attributes. First, roginolisib appears to stabilise PI3Kδ in an inactive conformation (Vadas et al, 2025. Manuscript co-submitted to Nature Communications). This binding mode renders roginolisib non-ATP competitive and confers high selectivity compared to other PI3K kinases[12,13]. Two unique residues in the C-terminal helix of the kinase domain stabilise the roginolisib-induced inactive conformation. This novel mode of inhibition and the resulting high selectivity is essential to minimise toxicities, as demonstrated by previous modelling studies[34]. Second, the PK profile of roginolisib confers the ability to dose continuously in patients. In animals the administration of roginolisib at doses above the threshold for selective PI3Kδ inhibition can lead to concomitant inhibition of PI3Kα and PI3Kβ at C_{max}. This co-inhibition is associated with the known gastrointestinal and hepatic toxicities and is avoided in patients at the BED[18]. The observed low to moderate variability in PK exposure and the low peak-to-trough ratio exhibit an important differentiation from the first-generation PI3Kδ inhibitors. Third, roginolisib has a favourable drug metabolism (DM) profile with no major active or reactive metabolites, all of which can interfere with selectivity or even induce idiosyncratic adverse events[35,36].

The unique safety and DMPK profile at the BED may have been a key factor for the anti-tumour responses and clinical benefit. Patients with NHL-FL had PRs at the 80 mg dose and not at the 20 mg dose. For patients with solid malignancies, there were 2 PRs, one in a patient with mCM (a patient with a BRAF mutation) and another with mUM. However, SD over several weeks of treatment can be an

indicator of clinical benefit, especially for immunotherapy as reported with tebentafusp treatment[37]. In patients with mUM, PFS and SD/PD at Week 16 were potential early predictive indicators of OS. Among the 29 mUM patients, the mOS was 20.8 months and at the final subsequent data-cut off (Dec 2024) the mOS was 15.9 months (Supplement Table S8). Post-roginolisib 17% of patients (5/29) received additional treatments, while the rest received supportive care. Thus, the OS was unlikely to be influenced by post-roginolisib treatments. The mOS of roginolisib exceeded the historical survival data (i.e., mOS of about 7 months) of mUM patients receiving 2nd /3rd line treatment[38]. Furthermore, the mOS of 15.9 months in mostly HLA-02:01-negative mUM patients (3/17) is comparable to 16.8 months reported for 2nd line HLA-02:01 positive patients treated with tebentafusp[39]. Other potential prognostic factors in the present FiH dose study were consistent with mUM patients treated in ≥ 2nd line: hepatic and extrahepatic disease (25/29; 86%); increased LDH (17/29; 59%) at baseline; characteristic mutations in *GNAQ* and *GNA11* genes.

To explore factors that may have contributed to the 15.9 months mOS and thus understand the underlying anti-tumour effects, we undertook several exploratory studies. Assessment of volumetric changes of all tumour lesions at Week 8 and 16 revealed a pattern of mixed responses. Also, the changes of the radiomic feature QCOD was another indicator of anti-tumour responses as previously reported[21]. The volumetric change of the spleen was not directly related to tumour responses or OS. Nevertheless, the change of this large immune organ indicates a pharmacologic response to roginolisib because most first-generation PI3Kδ inhibitors reduce spleen volumes as recently shown in patients with Activated PI3K delta syndrome (APDS) and treated with leniolisib[40]. These changes may be indicative of benefit to patients similar to the effects observed with ICI, where a reduction in spleen volume was associated with improved outcome [41].

Another possible indicator for anti-tumour effect of roginolisib were changes in immune cell dynamics, which were enhanced in patients who had SD at Week 16. At baseline, mUM patients had an immune suppressed phenotype (Supplemental Fig. 7). Immune suppressive cell populations were reduced during roginolisib treatment, such as Treg cells, $CD5^+$ B cells[42], $CD8^+CD39^-$ and $CD56^+CD16^-$ NK cells[43] indicating possible relief of immunosuppression. By contrast, activated $CD39^+CD8^+$ T cells increased, and their increase was positively correlated with improved OS (Fig. 3).

A third indicator of pharmacologic effect were changes in plasma proteins, mostly related to immune cell activation and the PI3K-mTOR pathway. We detected increases in IL-15, IL-17D and IFNGR2. All 3 are known to increase lymphocyte activity, especially after ICI treatment[44–46]. We also observed that immune suppressive $CD5^+$ B cells diminished during the same period as plasma soluble CD5 (sCD5) and soluble CD5-Ligand (sCD5L) levels decreased. Interestingly, soluble PD-1 (sPD-1) was reduced, a change reported previously for mCM patients responding to ICI[47]. Plasma proteins associated with the PI3K-mTOR pathway (i.e., FKBP4, AKT1S1, INPP5D, PIK3AP1) also changed, mainly in patients who had PD at Week 16 (Supplement Fig. 9). The origin of these detected proteins in the circulation remains unclear and will be re-evaluated in future clinical studies.

A fourth indicator of possible anti-tumour effect of roginolisib were changes in cfDNA in a subgroup of mUM patients (18/29; 62%). We used a tumour tissue agnostic approach and evaluated individual variants during treatment. Because of variability in the individual variants, we calculated the mean variant allele frequency of all impactful mutations of interest to better monitor changes over time[48]. While our data suggest that this approach can effectively track the changes in cfDNA, it may fail to capture genetically distinct metastatic clones.

Genomic and transcriptomic changes in tumour tissue provided an additional indication of roginolisib´s anti-tumour effect. In the tumour biopsies of mUM patients, constitutive activation of GPCRs were mostly found in patients with SD at Week 16 (Supplemental Fig. 9e). Gene Ontology (GO) pathway analysis revealed an enrichment of GPCRs, which included driver mutations, such as *GNAQ* and *GNA11*, known to cause constitutive activation of GPCR signalling[49]. Therefore, the signature of decreased GPCR, observed in on-treatment biopsies in our study, may suggest a favorable outcome in patients treated with roginolisib.

Lastly, the reduction of immune suppressive cells in tumour tissue mirrored the changes detected in the blood. Using multiplex IHC on 9 paired tumour biopsies demonstrated that the ratio of Treg cells to $CD8^+$ T cells shifted in favour of the $CD8^+$ T cells during roginolisib treatment (Fig. 5a-c). The changes were observed after 5 weeks of treatment and coincided with changes in peripheral blood and the concomitant spleen volume reduction.

In summary, this FiH dose study with roginolisib showed that selective inhibition of PI3Kδ in patients with a next generation inhibitor can reverse tumour-induced immune suppression. Continuous daily treatment was not accompanied with toxicities commonly associated with the first-generation PI3Kδ inhibitors. Thus, the favorable toxicity and DMPK profile allowed an uninterrupted inhibition of PI3Kδ. Correlative analyses across blood, plasma, and tumour biopsies consistently indicated reversal of conditions associated with tumour-induced immune suppression and engagement of $CD8^+$ T cells. Additional Phase 2 studies with randomised design are currently ongoing to further investigate the anti-tumour effects of roginolisib in different indications. In mUM, the ongoing randomised study (NCT06717126) is currently investigating the effect of roginolisib in mUM patients without a need to test their HLA status.

Methods

Clinical trial

This study was performed in accordance with ethical principles that have their origin in the Declaration of Helsinki and conducted in adherence to the study Protocol, Good Clinical Practices (GCP) as defined in International Council for Harmonisation of Technical Requirements for Pharmaceuticals for Human Use (ICH) GCP consolidated guidelines (E6) and applicable regulatory requirements. Each institution´s

review board approved the study and all patients signed an informed consent document before participation.

ClinicalTrials.gov registration number: NCT04328844 (registered March 30, 2020).

Participants

Based on the over-expression of PI3Kδ (PIK3CD) or a condition of immune suppression, patients with metastatic malignant mesothelioma, cutaneous and uveal melanoma malignancies participated in the study (Supplement Fig 1). A separate group of patients included patients with NHL-FL. Eligible patients were ≥ 18 years of age, with an Eastern Cooperative Oncology Group (ECOG) performance status (PS) of 0 to 1. For patients with NHL-FL, ECOG PS of 2 was allowed. All patients had to have a prior or recent histologic or cytologic confirmed diagnosis of advanced or metastatic malignancies and measurable disease. Patients with prior systemic therapy were required to have progressed or be intolerant to or refused treatment. Additional inclusion criteria, were specified for participants with cutaneous melanoma, ocular/uveal melanoma, advanced or metastatic mesothelioma or NHL-FL (see supplement protocol).

Study design

Roginolisib was evaluated in a two-part study. Part A was a dose escalation in patients with mUM, mCM, mesothelioma or NHL-FL. Part B was a dose expansion at the Biologically Effective Dose (BED) in mUM patients (Fig 1). Patients in Part A were evaluated for safety, PK and preliminary anti-tumour activity of roginolisib. In each dose cohort, PK and pharmacodynamic samples were collected and analysed to confirm the predicted non-clinical PK/pharmacodynamic model. In Part B, the BED determined from Part A was further evaluated in patients with mUM. Safety, PK and available pharmacodynamic data were examined and reviewed regularly by the Safety Monitoring Committee (SMC) and before escalating to the next dose.

Study drug treatment: dose and dose levels

Roginolisib hemi-fumarate was given once daily as a continuous dose and as part of a 28-day cycle. For patients with solid malignancies, doses started at 10 mg for Cohort 1, followed by 20 mg for Cohort 2, 40 mg for Cohort 3 and 80 mg for Cohort 4. Once the BED was established in patients with solid malignancies, the safety of the BED (or its range) was assessed in patients with NHL-FL.

Treatment

All patients were asked to use roginolisib at the prescribed dose and schedule. No dose adjustments or reductions were allowed for each dose level during the first 28 days to allow adequate safety and PK evaluation. Patients were to stop study treatment at any signs of medically significant toxicity as part of the safety evaluation. A compliance of at least 75% of drug administration during the first 28 days was

considered necessary for safety and PK evaluation. Treatment beyond progression (TBP) was allowed in case there were no tumour-progression related symptoms[50].

Safety assessment and maximum tolerated dose and dose-limiting toxicity assessment

Safety was evaluated in patients who received at least one dose of roginolisib and was based on summaries of adverse events (AE; CTCAE version 5.0), possible relatedness to roginolisib, dose limiting toxicities (DLTs), laboratory changes (including ALT, AST), changes in ECOG performance status, and changes in immune-related AEs. Unacceptable toxicity was defined as follows: (a) occurrence of an AE related to roginolisib that compromised the participant's ability to continue study-specific procedures, (b) an AE requiring more than two consecutive dose reductions; (c) Persistent AEs requiring a delay of therapy for more than 14 days; (d) concurrent elevation of ALT or AST >3×ULN and total bilirubin >2×ULN in patients who did not have causes that could be otherwise explained.

The maximum-tolerated dose (MTD) was defined as the dose level below which 2 patients (of up to 6 patients) experienced a DLT during cycle 1. If a DLT were to occur, the previous dose level was to be declared the MTD. Dose escalation to the next cohort proceeded only after: (i) 3 patients completed 1 treatment cycle of 28 days without a DLT; (ii) after assessment of their PK profile and meeting the pre-defined PK profile; (iii) complete safety assessment. At each dose level haematologic or non-haematologic drug-associated toxicity with Grade 3 was considered a DLT according to the National Cancer Institute and the Common Terminology Criteria for Adverse Events (CTCAE), version 5.0.

Response assessment

Radiographic changes (CR, PR, SD, PD) were evaluated by investigators using RECIST 1.1 (patients with solid malignancies) and Lugano criteria (patients with FL-NHL). Investigators reported lesion measurements in case report forms for subsequent statistical analyses. Patients with SD and PD at Week 16 based on RECIST 1.1. were used to differentiate two subpopulations.

Progression-free survival

PFS was summarised using the Kaplan-Meier product-limit method and displayed graphically using Kaplan-Meier plots. The PFS rate at 3, 6, 9 and 12 months, and corresponding 95% confidence intervals (CI), was also estimated using the Kaplan-Meier method.

Overall survival

OS was summarised using the Kaplan-Meier product-limit method and displayed graphically using a Kaplan-Meier plot. The OS rate at 3, 6, 9 and 12 months, and corresponding 95% CIs, was also estimated using the Kaplan-Meier method.

All data were reported to a data cut off of 20-December 2023. In addition, OS analysis for patients with mUM was also conducted with a data cut off 05-May-2024 for assessment of SD/PD correlations with

biomarkers and survival.

Burden of therapy

The Toxicity Units in the Burden of Therapy (BOTh) methodology measures the overall impact of adverse events (AEs) on patients during a clinical study. Instead of counting how many AEs occur, this approach takes into account the number, severity, and timing of events, giving a more meaningful view of how treatment affects patients.

The BOTh graph is generated using SAS®. It is a mirrored bar chart with study week on the x-axis and weighted AE burden on the y-axis, corrected for the number of subjects at risk. The following parameters are used:

1. Severity weighting: Each AE is assigned a weight based on its severity (Grade 1 = 1, Grade 2 = 2, etc.), so more severe AEs contribute more to the total burden.

2. Daily patient burden: For each patient, on each day of the study, the burden is calculated by summing the weighted AEs they experienced. This shows how much AEs affected them on that day.

3. Average daily burden across patients: To capture the group-level impact, the daily burdens are averaged across all patients at risk (i.e., still participating) on that day. This ensures patients who discontinued or completed treatment are not incorrectly included.

4. Weekly burden: These average daily burdens are then summed over a week, showing the cumulative weekly impact of AEs on patients.

Radiomics

Images acquired by a dedicated computer tomography (CT) scan machine were submitted for central radiologic review to assess quality for segmentation. Assessment of tumour volumes was initially performed by manual segmentation of all the lesions in all the organs on baselines and follow up CT scans for every 8 weeks (Week 8, Week 16 and Week 24). Patient response was evaluated based on changes in total tumour burden over time, determined by analysing volume differences in the 3D lesion segmentations at each timepoint. The percentage changes in tumour volume from baseline and the previous time-point were longitudinally compared to baseline with a response category scale.

Response category scales were calculated following recommendations from the RECIST working group[51] and the QIBA consortium[52]. The association of the final lesion response with the lesions' initial size was conducted[53]. Radiomic features are quantitative imaging biomarkers extracted from medical images using data-characterization algorithms. These features capture information about tumour intensity, shape, size, and texture, potentially providing a comprehensive quantitative description of tumour phenotypes[54]. Appearing lesions were excluded from this analysis to focus on the evolution of

existing tumours. Only lesions from lung and liver organs were considered to maintain consistency across patients.

Before conducting the feature reduction and statistical analyses, feature normalization was performed using the z-score method. Z-score normalization transforms each feature to have a mean of 0 and a standard deviation of 1. For each feature, the z-score was calculated as follows: $z = (x - \mu) / \sigma$. Where x is the original feature value, μ is the mean of the feature across all samples, and σ is the standard deviation of the feature across all samples. This normalization was performed separately for each feature in lungs and liver separately, across all time points. The following analyses were performed. (1) A Wilcoxon rank-sum test on selected baseline and delta radiomic features. (2) Features that passed feature reduction stages were included for multivariate analysis. (3) A generalised logistic regression model was fitted to predict the binary outcome (response vs. non-response) at Week 24. (4) To identify properties of lesions that may change over time in responsive or non-responsive lesions, a longitudinal evolution analysis was conducted using a Two-way Repeated Non-parametric ANOVA. (5) Since many features were compared, the Bonferroni correction was applied to control the overall Type I error rate. (6) For features showing significant effects, post-hoc pairwise comparisons were conducted to identify specific time points or groups where differences occurred.

Immunophenotyping of whole blood by mass cytometry

Purified antibodies were conjugated to metal isotopes as previously described[55,56]. Whole blood (WB) was obtained by phlebotomy after vein puncture and blood was collected in K2EDTA, 2 mL tubes. Then, samples were stabilised using whole blood cell stabiliser (Cytodelics AB) and stored at -80°C for future processing. After thawing, stabilised WB samples were fixed and lysed using the fix/lyse buffers provided in the whole blood processing kit (Cytodelics AB), transferred to 96-well plates, and cryopreserved at -80˚C. Fixed/lysed samples on 96-well plates were thawed, barcoded (using automation), and stained. Automation platform (Agilent, Santa Clara, CA, USA) was used for barcoding the samples. After barcoding, samples were pooled and blocked with FcR blocking buffer. Surface marker staining was performed with an antibody cocktail,cells were then washed and fixed with 2% PFA. The DNA intercalator Iridium 1000X was added to stain DNA. Cells were counted and the cell concentration was adjusted in each pooled sample batch tube to 750,000 cells/mL with CAS plus and to this 0.1X EQ6 normalization beads were added. Samples were acquired using the CyTOF XTTM (Standard BioTools Inc., USA). with event rate of 200 - 500 events/sec.

Fcs files obtained from acquiring multiplexed batches on CyTOF were first normalised to bead standards[57], then debarcoded and deconvoluted using a proprietary debarcoder algorithm. The deconvoluted data files were then renamed according to the annotation of samples and then manually gated using FlowJo v10 software to annotate all immune cell populations of interest. Samples with fewer than 1000 single cells were filtered out. The correlation coefficients (r) and p-values (p) were calculated between frequencies and time points using Spearman correlation. A linear mixed-effects model was used to describe the longitudinal changes in the frequencies of each cell subpopulation. The

time point was considered as the fixed effect and the subject identifier was considered as the random effect. The intercept of the model was allowed to vary for each subject so that the inter-individual differences were taken into consideration. ANOVA was then used to evaluate the p-value of the time point in the model. A p-value smaller than the significance level (0.05) represents a significant change in the cell subpopulation over time during treatment

Plasma – Olink

The protein expression was analysed from the plasma of patients, using the Olink Proximity Extension Assay (PEA). EDTA plasma samples were run on Olink's Explore 3072. The data for each protein are given as a normalised protein expression (NPX) value, an arbitrary unit on a Log2 scale and normalised to minimise both intra-assay and inter-assay variations.

Data was generated in two separate batches. To enable joint analysis of these two datasets, batch correction was applied to reduce the technical differences between these batches. The difference of medians method was applied as implemented in the olink_normalization_subset function. The Sidak adjusted p-values were calculated by Analysis of Variance (ANOVA) and linear mixed effects (lmer) model. The individual proteins (23/29 patients) over time were analysed using R Studio software (2024.09.0 +375) and the OlinkAnalyze package (https://github.com/Olink-Proteomics/OlinkRPackage). The heatmap was generated by plotting the relative expression values for 3 cycles (C2D1, C3D1, C4D1) compared to baseline (C1D1). Only the 83 significative proteins were represented in a heatmap using GraphPad Prism (V10.2.3).

Multiplex immunohistochemistry

Microscope Axio Lab (Zeiss, Oberkochen, Germany) with Bandpass filters (AHF Analysetechnik, Tübingen, Germany) were used to assess slides. Bond research tools were used (Leica Biosystems, Nussloch, Germany) to stain slides.

Formalin-Fixed Paraffin-Embedded (FFPE) tissue samples were sliced into 3 µm sections and mounted on TOMO Adhesion slides (VWR, Matsunami Glass, Bellingham, WA, USA) for IHC and Microscope glass slides (Medite GmbH, Burgdorf, Germany) were used for haematoxylin & eosin (H&E) staining. The following first primary antibodies were used in antibody dilution buffer (DCS): rabbit anti-CD8 clone SP16 at 1:225 dilution; rabbit anti-FOXP3 antibody clone SP97 at dilution of 1:137.6; rabbit anti-CD3 antibody clone 2GV6 at dilution of 1:1.3; mouse anti- Pmel17 antibody clone HMB45 at dilution 1:60. Staining was performed using reagents from the Opal 4-Color Automation IHC Kit (Akoya Biosciences, Marlborough, MA, USA), including the Opal 520 (for CD8) and Opal 570 fluorophores (for Pmel17), Opal 650 Reagent Pack (for CD3) and the TSA Plus Biotin Kit (for FOXP3) in combination with AF750 Streptavidin (Thermo Fisher Scientific, Waltham, MA USA). Cell nuclei were counterstained with DAPI (Opal 4-Color Automation IHC Kit, Akoya Biosciences). Scans were generated with the Axio Scan.Z1 automated slide scanner (Zeiss) using ZEN 3.1 (blue edition) slide scan software (Zeiss) and the Colibri 7 light source (Zeiss) for fluorophore excitation.

Tissue and Plasma (cell-free DNA and cfRNA) (Caris Life Sciences)

Next-generation sequencing analysis of DNA and RNA extracted from plasma and white blood cells (buffy coat) was performed using Illumina NovaSeq 6000 Sequencer (Illumina, San Diego, CA, USA). A hybrid pull-down panel of baits was used to capture DNA and reverse-transcribed RNA from >20,000 genes.

Samples were processed and WES was performed by Caris Life Sciences. The solid and liquid samples from mUM patients before and after treatment, were processed by Caris. Raw BAM files were obtained from Caris. VCF tables containing the variant calling analysis were subsequently generated by running the Sarek nextflow analysis pipeline (nf-core/sarek, version 3.4.0) to detect somatic variants. A filtering step was then performed to only select the variants meeting quality control standards, and removing mutations from unwanted sources such as: sequencing errors, technical artefacts and non-somatic mutations. SnpSift was used to retain only these high-quality variants. Finally, a conversion to tabular format was performed to extract specific fields such as allele frequency, chromosome, position and variant effect using bcftools query and awk.

Cell free (cfDNA) status for selected patients at Week 8 and\or Week 16 has been collected. The cfDNA was assessed using the Caris Assure Assay (Caris Assure™ blood-based profiling, Caris Life Sciences)[58]. Variants were first filtered to remove genes with a read depth of less than 5. Subsequently, only genes harbouring variants with moderate or high predicted mutational impact were retained for analysis. For each gene, the average variant allele fraction (VAFmean) was calculated across all remaining variants[59]. Transcriptomic analysis was conducted with the aim to analyse roginolisib's effect on gene expression, before and after treatment and between patients with stable disease (SD) and those with progressive disease (PD) at Week 16.

Tissue biopsies collected from uveal melanoma patients before and after treatment were processed to obtain DNA and RNA as previously described by Caris Life Sciences[60].

PRO-CTCAE

The Patient Reported Outcomes version of the Common Terminology Criteria for Adverse Events (PRO-CTCAE) was developed as a companion to the CTCAE and includes 78 symptomatic AEs with each AE characterised by presence (P), frequency (F), severity (S) and/or interference (I) for a total of 124 items[61]. From this library, 17 AEs (31 total items) were selected based on: (1) general oncology symptoms (fatigue (SI), general pain (FSI), headache (FSI), sad (FSI); (2) toxicities associated with first-generation PI3K inhibitors (abdominal pain (FSI), diarrhoea (F), itching (S), nausea (FS), rash (P), skin dryness (S), vomiting (FS)) and (3) toxicities potentially related to roginolisib (blurred vision (SI), dizziness (SI), flashing lights (P), numbness and tingling (SI), taste changes (S), visual floaters(P)). PRO-CTCAE assessments were completed on a mobile device (Castor™, The Netherlands) by patients at Screening, Cycle 1 Day 1, Cycle 1 Day 15, Cycles 2-25 and End-of-Treatment (EOT).

Statistical analyses for clinical data

Patient disposition, demographics, and disease characteristics, safety, concomitant medication and response data were summarised by study part, using line plots to investigate trends over time, waterfall plots for change in lesion size based on investigator-reported measurements (using RECIST 1.1 and Lugano criteria), summary statistics or frequencies as appropriate. Patients who received at least one dose of roginolisib were evaluated as part of the safety population. The efficacy population was defined as all participants who received at least one dose of roginolisib, had a baseline tumour assessment with measurable disease and had at least one of the following (a) At least one on-treatment tumour evaluation; (b) Had no clinical progression before the first on-treatment tumour assessment; (c) No death before the first on-treatment tumour assessment. The efficacy population was used for efficacy analysis or anti-tumour responses assessment. For details, please, see the attached Statistical Analysis Plan.

Declarations

Data Availability

Source data are provided with this paper in the supplementary material. The raw clinical data and genomics are available under restricted access due to privacy laws. Access to de-identified data can be obtained via written request that specifies the intended use of the data made to the corresponding author.

Acknowledgements

The authors thank the patients and their families. Further, we thank study personal at the clinical investigation centres, the Fortrea/LabCorp Drug Development team and Veramed (UK) for their statistical support.

For the multiplex IHC, we thank Indivumed GmbH (Falkenried 88, Bldg. D D-20251 Hamburg, Germany) for performing the assays.

The study at the Glasgow, UK, site was supported by the Glasgow Experimental Cancer Medicine Centre, funded by Cancer Research UK and the Chief Scientist's Office, Scotland.

Medical writing support was provided by Dr Gareth Hardy of Niche Science and Technology Ltd, Richmond-Upon-Thames, London, UK

Clinical trial identification

NCT: NCT04328844.

Funding and legal responsibility

The study Sponsor (iOnctura SA) funded the study and had full oversight of the study. The Sponsor was the legal entity responsible for the study.

Ethics declarations

Competing interests

M.L., G.D.C., L.V.V., A.B., P.K. and T.H. are employees of the study Sponsor (iOnctura) with stock options.

R.Z. is an employee of the study Sponsor (iOnctura).

A.M.D. is an investigator for MSD, Bristol Myers Squibb, Incyte, Pierre Fabre, Novartis, SunPharma, Immunocore, Sanofi and Servier and receives consulting fees and/or speaker fees/honoraria and/or research funding from Bristol Myers Squibb, Roche, Sanofi, Pierre Fabre, GlaxoSmithKline and Vyvamed.

M.S. sits on advisory boards for Servier, Incyte, GlaxoSmithKline and Bristol Myers Squibb, receives travel grants for Pfizer, Sanofi, Roche, Servier and BeOne and receives consulting fees and/or speaker fees/honoraria and/or research funding from GlaxoSmithKline and Bristol Myers Squibb.

P.S. is a speaker for Bristol Myers Squibb, sits on advisory boards for Iovance Biotherapeutics and Sun Pharma, is an investigator for Accession Therapeutics, BioNTech, C4 Therapeutics, Corvus Pharmaceuticals, Ideaya Biosciences, Immunocore, Iovance Biotherapeutics, Microbiotica, Moderna, Mythic and for Eisai.

M.V. is an investigator for Novartis.

P.B. and T.L. are shareholders and cofounders of Cytodelics AB which produce and distribute whole blood cell stabiliser solutions used within this study.

P.B. is scientific advisor to Pixelgen Technologies AB, Sention Health AB, Helaina Inc., Scailyte AG, and Oxford Immune Algorithmics, holds shares with Pixelgen Technologies, Sention Health, Infinant Health, Single Technologies and AstraZeneca and is a speaker for Nestlé, Sobi, AstraZeneca, Pfizer and CSL Behring.

M.D. is an employee of Fortrea with stock options.

A.C. and N.S. are employed by radiomics.bio consultancy with stock options.

M.O. receives consulting fees and/or speaker fees/honoraria and/or research funding from radiomics.bio.

R.S. is employed of Astellas.

A.A.A. is an employee of BOTh Analytics.

A.M, U.P. and G.P. receive consulting fees and/or speaker fees/honoraria and/or research funding from the study sponsor (iOnctura).

G.H and E.W. are employees of Veramed.

V.V. and A.L.P are employees of 4HF Biotec GmbH and have stock options with APEX OncoScience SAS.

M.P. and D.S. are employees of Caris Life Sciences with stock options.

C.C.S. sits on an advisory boards for ADC Therapeutics, Karyopharm Tx, Bristol Myers Squibb, Roche, MSD, Scenic Biotech, Sobi, Abbvie and Genmab and receives consulting fees and/or speaker fees/honoraria and/or research funding from Sanofi, ADC Therapeutics, Bristol Myers Squibb, Incyte, Roche, Janssen Oncology, Takeda, MSD, AstraZeneca and Gilead.

A.S. is employed by IRCCS Humanitas Research Hospital, is a speaker for Takeda, Bristol Myers Squibb, Roche, Abbvie, Amgen, Celgene, Servier, Gilead, AstraZeneca, Pfizer, Arqule, Lilly, Sandoz, Eisai, Novartis, Bayer, MSD and Beigene, sits on advisory boards for Bristol Myers Squibb, Servier, Gilead, Pfizer, Eisai, Bayer and MSD and receives consulting fees and/or speaker fees/honoraria and/or research funding from Sanofi and Incyte.

T.H.E. receives travel grants from Bristol Myers Squibb, MSD, Pierre Fabre, Eisai, Nucana and Roche and receives consulting fees and/or speaker fees/honoraria and/or research funding from the study sponsor (iOnctura), Karus Therapeutics, Eisai, Bristol Myers Squibb, MSD, United Medical, Nucana, Roche/Genentech, Ascelia, AstraZeneca, Bicycle Therapeutics, Medivir, Seagen, CV6 Therapeutics, Ewopharma, Beigene, Basilea, Celgene, MiNA Therapeutics, Lilly, Merck Serono, Janssen, Johnson & Johnson, Verastem, Novartis, Iovance Biotherapeutics, Sanofi/Aventis, Clovis Oncology, Plexxikon, Sierra Pharma, GlaxoSmithKline, Halozyme, CytomX Therapeutics, Vertex, Athenex, Adaptimmune, Immunocore, Modulate Pharma, Berg, Starpharma, BiolineRx, UCB, Sapience Therapeutics, Astellas Pharma, Boehringer Ingelheim, Avacta Life Sciences, Nurix, Codiak BioSciences, T3 Pharmaceuticals, BioNTech, Moderna Therapeutics, Exelixis, Exscientia, Bayer, Amgen, Sotio and Pfizer.

M.M. owns stock in Epigen Therapeutics and Theravance, sits on advisory boards for MSD, Roche and Bristol Myers Squibb and receives consulting fees and/or speaker fees/honoraria and/or research funding from the study sponsor (iOnctura), MSD, Roche, Bristol Myers Squibb, Sanofi, AstraZeneca, Amgen, Pierre Fabre, Eli Lilly, GlaxoSmithKline, Sciclone, Alfasigma and Merck Serono.

Contributions

Each author has approved the submitted version (and any substantially modified version) of this manuscript. A.M.D., M.S., P.B., M.L., G.D.C., R.Z., L.V.V., P.K., T.H., E.W., C.C.S., A.S., T.H.E. and M.M each contributed to the conception or design of the work, data acquisition and analysis, interpretation of data and to drafting or revising the work. A.L., V.D.A., G.A. and M.V. each contributed to the conception or design of the work and to data acquisition and analysis. P.S. contributed to the conception or design of

the work, data acquisition and analysis and to drafting or revising the work. H.B., A.J. and L.G., M.D. and J.G. contributed to data acquisition and analysis and to interpretation of data. T.Z., T.L., A.C., N.S., M.O., R.S., A.A.A., A.M, U.P., G.P., G.H, V.V., A.L.P. M.P. and D.S. each contributed to data acquisition and analysis, interpretation of data and to drafting or revising the work. A.B. contributed to interpretation of data and to drafting or revising the work.

Corresponding author

Correspondence to: Author-40

Supplementary Information

Supplementary Information is combined and supplied as a separate file.

References

1. Vanhaesebroeck B, Perry MWD, Brown JR, Andre F, Okkenhaug K (2021) PI3K inhibitors are finally coming of age. Nat Rev Drug Discov 20:741–769
2. Cantley LC (2002) The phosphoinositide 3-kinase pathway. Science 296:1655–1657
3. Vanhaesebroeck B et al (1997) P110delta, a novel phosphoinositide 3-kinase in leukocytes. Proc Natl Acad Sci U S A 94:4330–4335
4. Brown JR, Danilov AV, LaCasce AS, Davids MS (2022) PI3K inhibitors in haematological malignancies. Lancet Oncol 23:e364
5. Goulielmaki E et al (2018) Pharmacological inactivation of the PI3K p110delta prevents breast tumour progression by targeting cancer cells and macrophages. Cell Death Dis 9:678
6. Okkenhaug K, Vanhaesebroeck B (2003) PI3K in lymphocyte development, differentiation and activation. Nat Rev Immunol 3:317–330
7. Ali K et al (2014) Inactivation of PI(3)K p110delta breaks regulatory T-cell-mediated immune tolerance to cancer. Nature 510:407–411
8. Whitehead MA, Bombardieri M, Pitzalis C, Vanhaesebroeck B (2012) Isoform-selective induction of human p110delta PI3K expression by TNFalpha: identification of a new and inducible PIK3CD promoter. Biochem J 443:857–867
9. Ahmad S et al (2017) Differential PI3Kdelta Signaling in CD4(+) T-cell Subsets Enables Selective Targeting of T Regulatory Cells to Enhance Cancer Immunotherapy. Cancer Res 77:1892–1904
10. Liu Y, Wan WZ, Li Y, Zhou GL, Liu XG (2017) Recent development of ATP-competitive small molecule phosphatidylinostitol-3-kinase inhibitors as anticancer agents. Oncotarget 8:7181–7200
11. Kirkland LO, McInnes C (2009) Non-ATP competitive protein kinase inhibitors as anti-tumor therapeutics. Biochem Pharmacol 77:1561–1571
12. Johnson Z et al (2023) IOA-244 is a Non-ATP-competitive, Highly Selective, Tolerable PI3K Delta Inhibitor That Targets Solid Tumors and Breaks Immune Tolerance. Cancer Res Commun 3:576–591

13. Haselmayer P et al (2014) Characterization of Novel PI3Kdelta Inhibitors as Potential Therapeutics for SLE and Lupus Nephritis in Pre-Clinical Studies. Front Immunol 5:233
14. Kalla C et al (2024) The highly selective and oral phosphoinositide 3-kinase delta (PI3K-delta) inhibitor roginolisib induces apoptosis in mesothelioma cells and increases immune effector cell composition. Transl Oncol 43:101857
15. Sasi BK et al (2025) Novel PI3kdelta inhibitor roginolisib synergizes with venetoclax in hematologic malignancies. Haematologica
16. Moreno O et al (2018) Pharmacokinetics, and Pharmacodynamics of ME-401, an Oral, Potent, and Selective Inhibitor of Phosphatidylinositol 3-Kinase P110delta, Following Single Ascending Dose Administration to Healthy Volunteers. Clin Ther 40:1855–1867Safety
17. Mellen PL, Morton SJ, Shields CL (2013) American joint committee on cancer staging of uveal melanoma. Oman J Ophthalmol 6:116–118
18. van der Veen L, Schmitt M, Deken MA, Lahn M (2023) Non-Clinical Toxicology Evaluation of the Novel Non-ATP Competitive Oral PI3 Kinase Delta Inhibitor Roginolisib. Int J Toxicol 42:515–534
19. Santos AF, Alpan O, Hoffmann HJ (2021) Basophil activation test: Mechanisms and considerations for use in clinical trials and clinical practice. Allergy 76:2420–2432
20. Zwanenburg A et al (2020) The Image Biomarker Standardization Initiative: Standardized Quantitative Radiomics for High-Throughput Image-based Phenotyping. Radiology 295:328–338
21. Grossmann P et al (2017) Defining the biological basis of radiomic phenotypes in lung cancer. Elife 6
22. Chow A et al (2023) The ectonucleotidase CD39 identifies tumor-reactive CD8(+) T cells predictive of immune checkpoint blockade efficacy in human lung cancer. Immunity 56:93–106e106
23. Gadi D et al (2022) Idelalisib reduces regulatory T cells and activates T helper 17 cell differentiation in relapsed refractory patients with chronic lymphocytic leukaemia. Br J Haematol 197:207–211
24. Rapp M et al (2019) CCL22 controls immunity by promoting regulatory T cell communication with dendritic cells in lymph nodes. J Exp Med 216:1170–1181
25. Landreville S et al (2011) Identification of differentially expressed genes in uveal melanoma using suppressive subtractive hybridization. Mol Vis 17:1324–1333
26. Castel P, Toska E, Engelman JA, Scaltriti M (2021) The present and future of PI3K inhibitors for cancer therapy. Nat Cancer 2:587–597
27. Ali K et al (2004) Essential role for the p110delta phosphoinositide 3-kinase in the allergic response. Nature 431:1007–1011
28. Skanland SS, Okkenhaug K, Davids MS (2024) PI3K Inhibitors in Hematology: When One Door Closes. Clin Cancer Res 30:3667–3675
29. Borazanci E et al (2020) A Phase Ib Study of Single-Agent Idelalisib Followed by Idelalisib in Combination with Chemotherapy in Patients with Metastatic Pancreatic Ductal Adenocarcinoma. Oncologist 25:e1604–e1613

30. Eschweiler S et al (2022) Intermittent PI3Kdelta inhibition sustains anti-tumour immunity and curbs irAEs. Nature 605:741–746
31. Munster P et al (2023) Combination of Itacitinib or Parsaclisib with Pembrolizumab in Patients with Advanced Solid Tumors: A Phase I Study. Cancer Res Commun 3:2572–2584
32. Hanlon A, Brander DM (2020) Managing toxicities of phosphatidylinositol-3-kinase (PI3K) inhibitors. *Hematology Am Soc Hematol Educ Program* 346–356 (2020)
33. Kulbay M et al (2024) Uveal Melanoma: Comprehensive Review of Its Pathophysiology, Diagnosis, Treatment, and Future Perspectives. *Biomedicines* 12
34. Gadkar K et al (2021) Quantitative systems pharmacology model-based investigation of adverse gastrointestinal events associated with prolonged treatment with PI3-kinase inhibitors. CPT Pharmacometrics Syst Pharmacol
35. Zhu J et al (2018) Identification of Novel Pathways in Idelalisib Metabolism and Bioactivation. Chem Res Toxicol 31:548–555
36. Cho T, Uetrecht J (2017) How Reactive Metabolites Induce an Immune Response That Sometimes Leads to an Idiosyncratic Drug Reaction. Chem Res Toxicol 30:295–314
37. Nathan P et al (2021) Overall Survival Benefit with Tebentafusp in Metastatic Uveal Melanoma. N Engl J Med 385:1196–1206
38. Rantala ES, Hernberg M, Kivela TT (2019) Overall survival after treatment for metastatic uveal melanoma: a systematic review and meta-analysis. Melanoma Res 29:561–568
39. Carvajal RD et al (2022) Clinical and molecular response to tebentafusp in previously treated patients with metastatic uveal melanoma: a phase 2 trial. Nat Med 28:2364–2373
40. Rao VK et al (2023) A randomized, placebo-controlled phase 3 trial of the PI3Kdelta inhibitor leniolisib for activated PI3Kdelta syndrome. Blood 141:971–983
41. Galland L et al (2021) Splenic Volume as a Surrogate Marker of Immune Checkpoint Inhibitor Efficacy in Metastatic Non Small Cell Lung Cancer. Cancers (Basel) 13
42. Taher TE et al (2020) CD5 and B lymphocyte responses: multifaceted effects through multitudes of pathways and channels. Cell Mol Immunol 17:1201–1203
43. de Jonge K et al (2019) Circulating CD56(bright) NK cells inversely correlate with survival of melanoma patients. Sci Rep 9:4487
44. Saddawi-Konefka R et al (2016) Nrf2 Induces IL-17D to Mediate Tumor and Virus Surveillance. Cell Rep 16:2348–2358
45. Liu X, Sun S, Liu D (2020) IL-17D: A Less Studied Cytokine of IL-17 Family. Int Arch Allergy Immunol 181:618–623
46. Williams JB et al (2020) Tumor heterogeneity and clonal cooperation influence the immune selection of IFN-gamma-signaling mutant cancer cells. Nat Commun 11:602
47. Pedersen JG et al (2022) Increased Soluble PD-1 Predicts Response to Nivolumab plus Ipilimumab in Melanoma. Cancers (Basel) 14

48. Rodrigues M et al (2024) Prospective assessment of circulating tumor DNA in patients with metastatic uveal melanoma treated with tebentafusp. Nat Commun 15:8851
49. O'Hayre M et al (2013) The emerging mutational landscape of G proteins and G-protein-coupled receptors in cancer. Nat Rev Cancer 13:412–424
50. Beaver JA et al (2018) Patients with melanoma treated with an anti-PD-1 antibody beyond RECIST progression: a US Food and Drug Administration pooled analysis. Lancet Oncol 19:229–239
51. Eisenhauer EA et al (2009) New response evaluation criteria in solid tumours: revised RECIST guideline (version 1.1). Eur J Cancer 45:228–247
52. QIBA. CT Tumor Volume Change for Advanced Disease, Clinically Feasible Profile. (ed. Committee, C.V.B.) (Version: Stage 3: Clinically Feasible (Publication date: 2022 July) (2022)
53. Eskelin S, Pyrhonen S, Hahka-Kemppinen M, Tuomaala S, Kivela T (2003) A prognostic model and staging for metastatic uveal melanoma. Cancer 97:465–475
54. Lambin P et al (2012) Radiomics: extracting more information from medical images using advanced feature analysis. Eur J Cancer 48:441–446
55. Lakshmikanth T, Brodin P (1913) Systems-Level Immune Monitoring by Mass Cytometry. *Methods Mol Biol* 33–48 (2019)
56. Chen Q et al (2025) Systems-level immunomonitoring in children with solid tumors to enable precision medicine. Cell 188:1425–1440e1411
57. Finck R et al (2013) Normalization of mass cytometry data with bead standards. Cytometry A 83:483–494
58. Abraham J et al (2025) Validation of an AI-enabled exome/transcriptome liquid biopsy platform for early detection, MRD, disease monitoring, and therapy selection for solid tumors. Sci Rep 15:21173
59. Fujii Y et al (2021) Identification and monitoring of mutations in circulating cell-free tumor DNA in hepatocellular carcinoma treated with lenvatinib. J Experimental Clin Cancer Res 40:215
60. Domenyuk V et al (2025) Clinical and analytical validation of MI Cancer Seek(R), a companion diagnostic whole exome and whole transcriptome sequencing-based comprehensive molecular profiling assay. Oncotarget 16:642–659
61. Basch E et al (2014) Development of the National Cancer Institute's patient-reported outcomes version of the common terminology criteria for adverse events (PRO-CTCAE). J Natl Cancer Inst 106

Figures

Figure 1

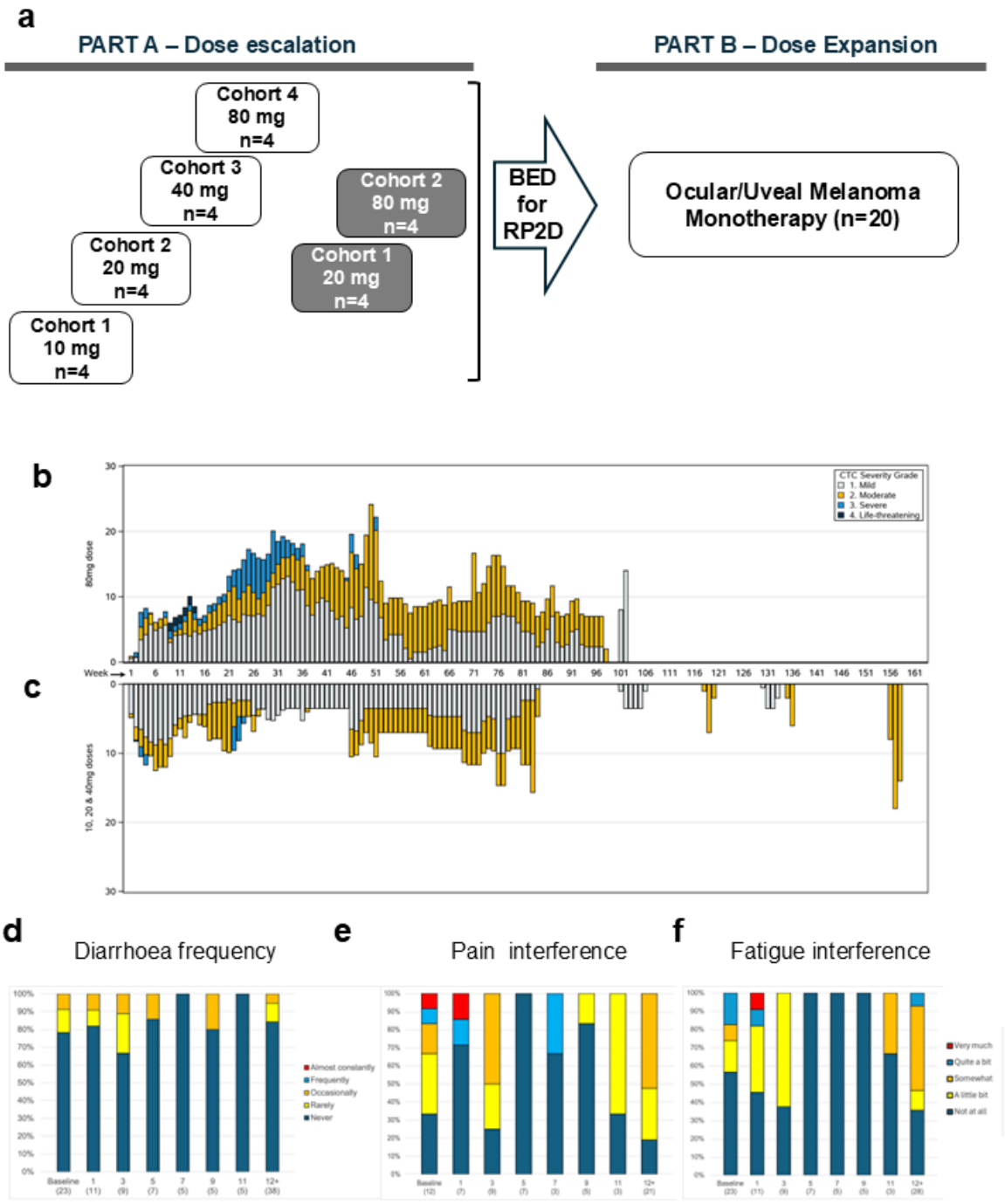


Figure 1

a Clinical study design layout. **b** Burden of Therapy (BoTh) in Study IOA-244-101 comparing **b** 80 mg QD to **c**doses of 10 to 40 mg. Y-axis: toxicity units quantify the cumulative impact of a patient's adverse effects during treatment (x-axis). Common severity of toxicities are separated in: 'Mild, Moderate, Severe and Life-threatening'. **d-f**Patient-reported Common Terminology Criteria for Adverse Events (PRO-

CTCAE) for diarrhoea (**d**), pain interference (**e**) and fatigue interference (**f**) show trends towards improvement up to Cycle 5. RP2D=recommended Phase 2 dose.

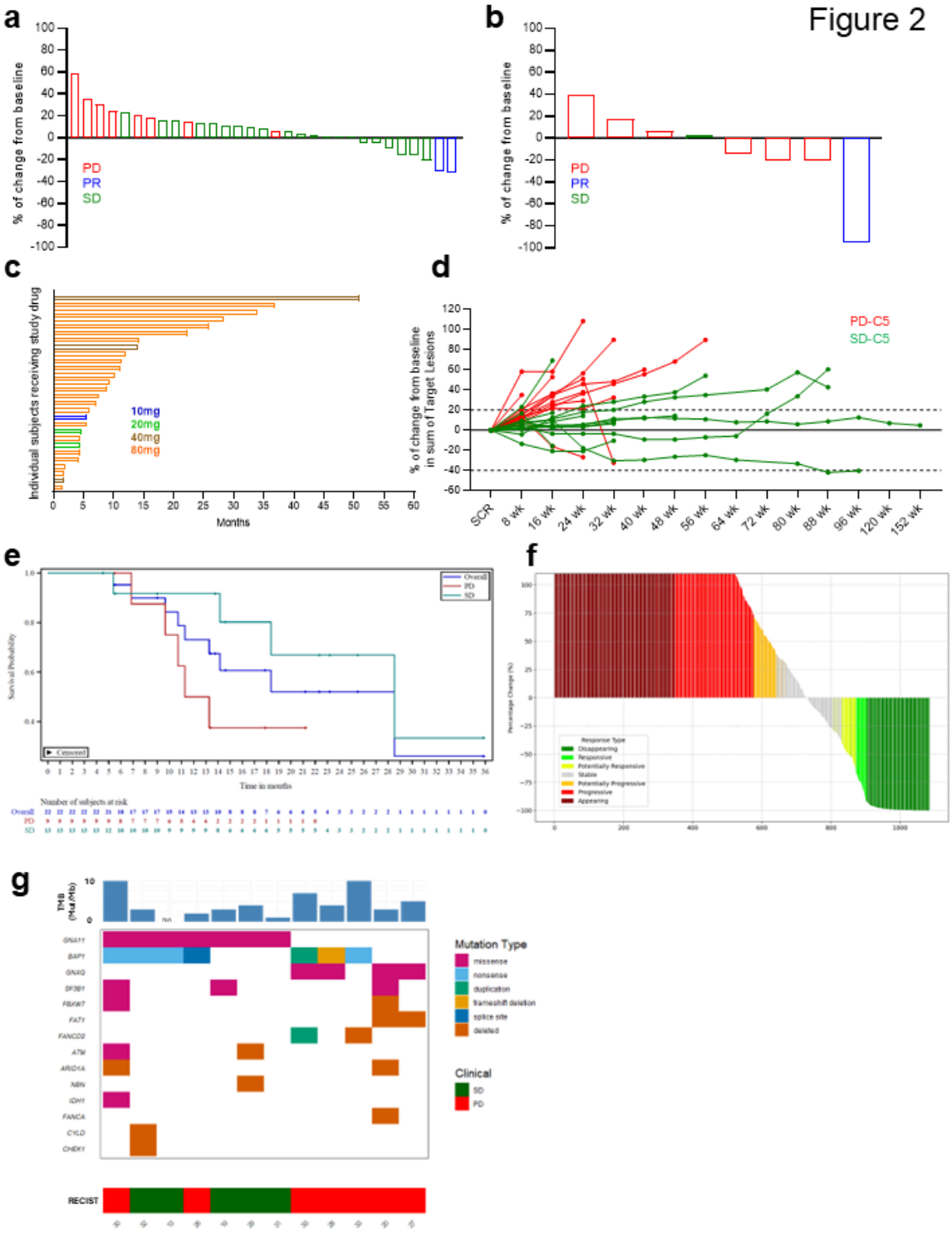


Figure 2

a Waterfall plots of best percentage changes from baseline for solid tumour patients (n=32) based on RECIST 1.1, and **b** for NHL-FL patients (n=8) based on Lugano 2014 criteria: PD; PR and SD). Baseline

was the most recent assessment prior to the first administration of roginolisib [Percentage change=100 × (value at the post-baseline visit – baseline value)/baseline value] **c** Time mUM patients were treated with roginolisib treatment at different doses (n=28). **d**Clinical benefit: percentage changes from baseline of Sum of Lesion Diameters (SLD) over time, separated by RECIST1.1 response at Week 16 (SD-C5 vs PD-C5) for each participant with mUM (n=28) (SCR= screening). **e** Kaplan–Meier analysis showing OS of patients (n=22) separated by RECIST1.1 and response at Week 16 (SD vs PD). **f** Percentage of change in tumour lesions measured by radiomics-based CT scans. **g**Oncoplot of mutations in mUM patients found in tumoral tissue (n=12) by whole exome sequencing and separated by response at Week 16 (SD vs PD) (TMB=Tumour Mutational Burden).

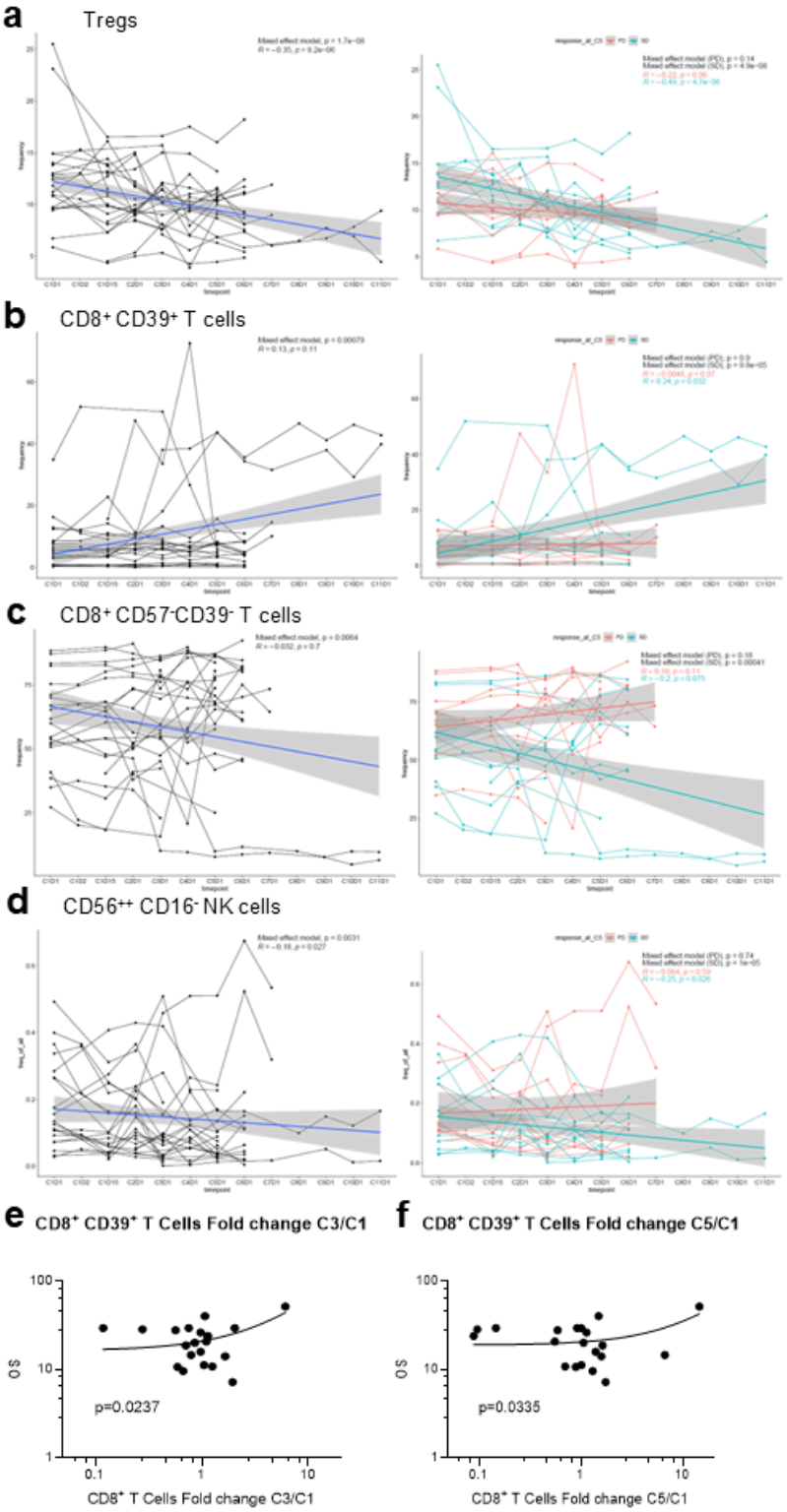


Figure 3

Figure 3

a Percentage of regulatory T cells (Treg) out of $CD4^+$ cells (Tregs, $CD4^+CD25^+CD127^{low}$), **b-c** cytotoxic $CD8^+$ T cells ($CD8^+CD39^+$; $CD8^+CD57^-CD39^-$) out of $CD8^+$ and **d** NK cells ($CD56^{++}CD16^-$) out of all cells in the blood of mUM patients (n=22) measured at different timepoints by mass cytometry and separated by disease progression. Line plots show the individual cell population levels during roginolisib treatment, and the correlations were evaluated using Spearman correlation coefficients (R) and their associated p-

values. In addition, mixed-effects model calculations were performed where patient identifiers (i.e., patient_ID) were considered as random effects using the R formula "subpop_frequency ~ timepoint + (1|patient_ID) (CxDx=Cycle x Day x). **d-f** Correlation between the OS of patients (n=20) and the fold change of the percentage of $CD39^{+}CD8^{+}$ T cells at **e** Cycle 3 compared to Cycle 1 and **f** Cycle 5 compared to Cycle 1.

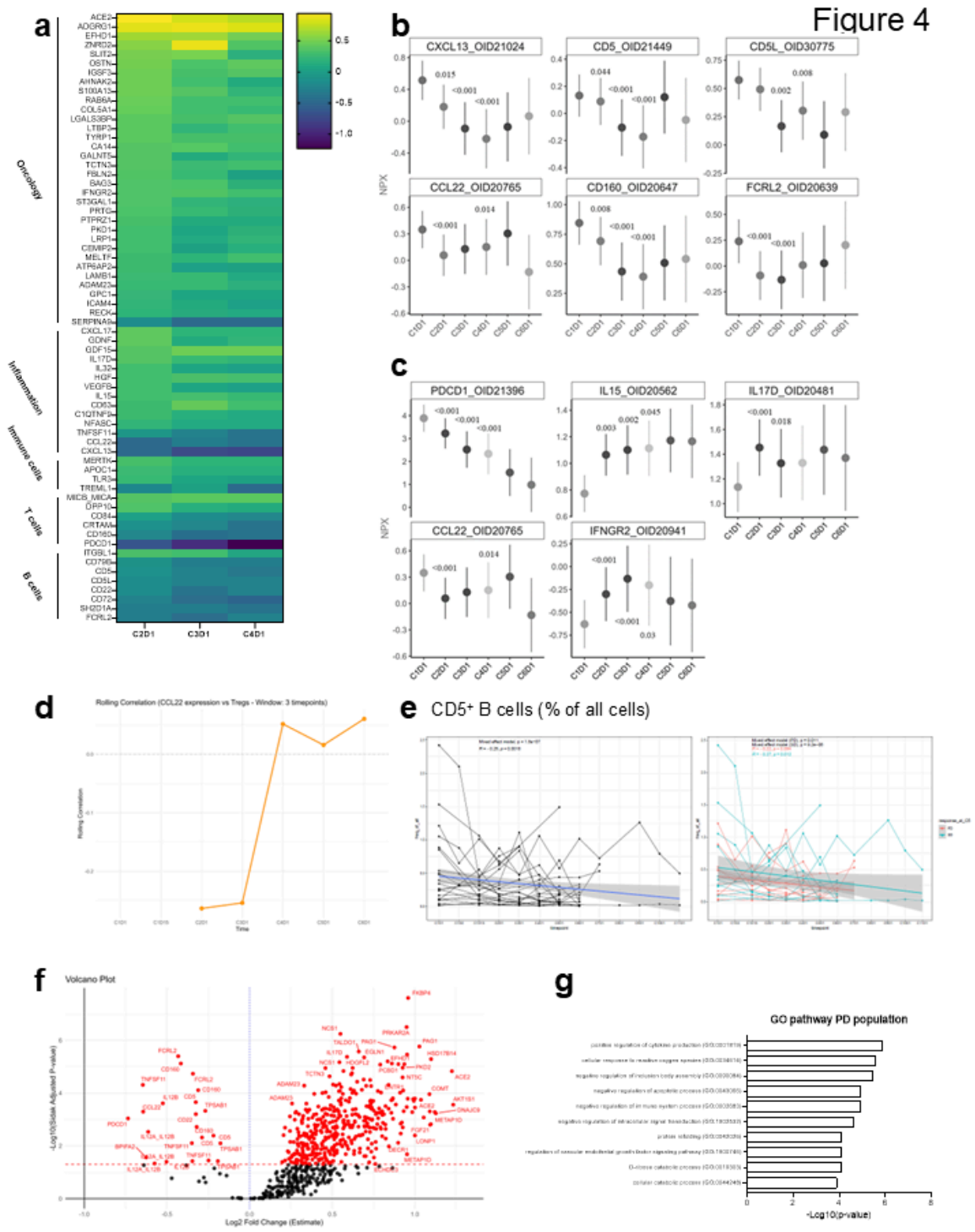


Figure 4

a Heatmap of proteins significantly regulated in the blood of mUM patients (n=29) treated with 80 mg of roginolisib measured by Olink assay and represented at Cycles 2, 3 and 4 compared to baseline. The Sidak adjusted p-values were calculated by Analysis of Variance (ANOVA) and linear mixed effects (lmer) model. Only significant proteins are represented. **b-c** Expression levels of proteins (NPX) involved in T cell or B cell biology and/or that have previously been reported as being modulated by other PI3Kδ inhibitors, measured by Olink assay. The Sidak adjusted p-values were calculated by ANOVA and lmer model (n=29). **d** Rolling correlation between CCL22 plasma levels and Tregs percentage calculated by Pearson's correlation coefficients at each time point in mUM patients (n=29). To assess temporal trends, these correlations were then smoothed using a rolling mean over consecutive time windows. **e** Percentage of $CD5^+$ B cells out of $CD45^+$ cells in the blood of mUM patients (n=22) measured at different timepoints by mass cytometry and separated by disease progression. The correlation coefficients (r) and p-values (p) (unadjusted) were calculated between frequencies and timepoints using Spearman correlation. Linear mixed effect model was used to describe the longitudinal changes of the frequencies of each cell subpopulation. **f** Volcano plot of differentially regulated proteins after roginolisib treatment in patients with PD at Week 16 (16/29). The Sidak adjusted p-values were calculated by Analysis of Variance (ANOVA) and linear mixed effects (lmer) model. **g** Gene ontology pathway analysis showed genes significantly upregulated in patients with PD at Week 16 as early as Cycle 3 (16/29).

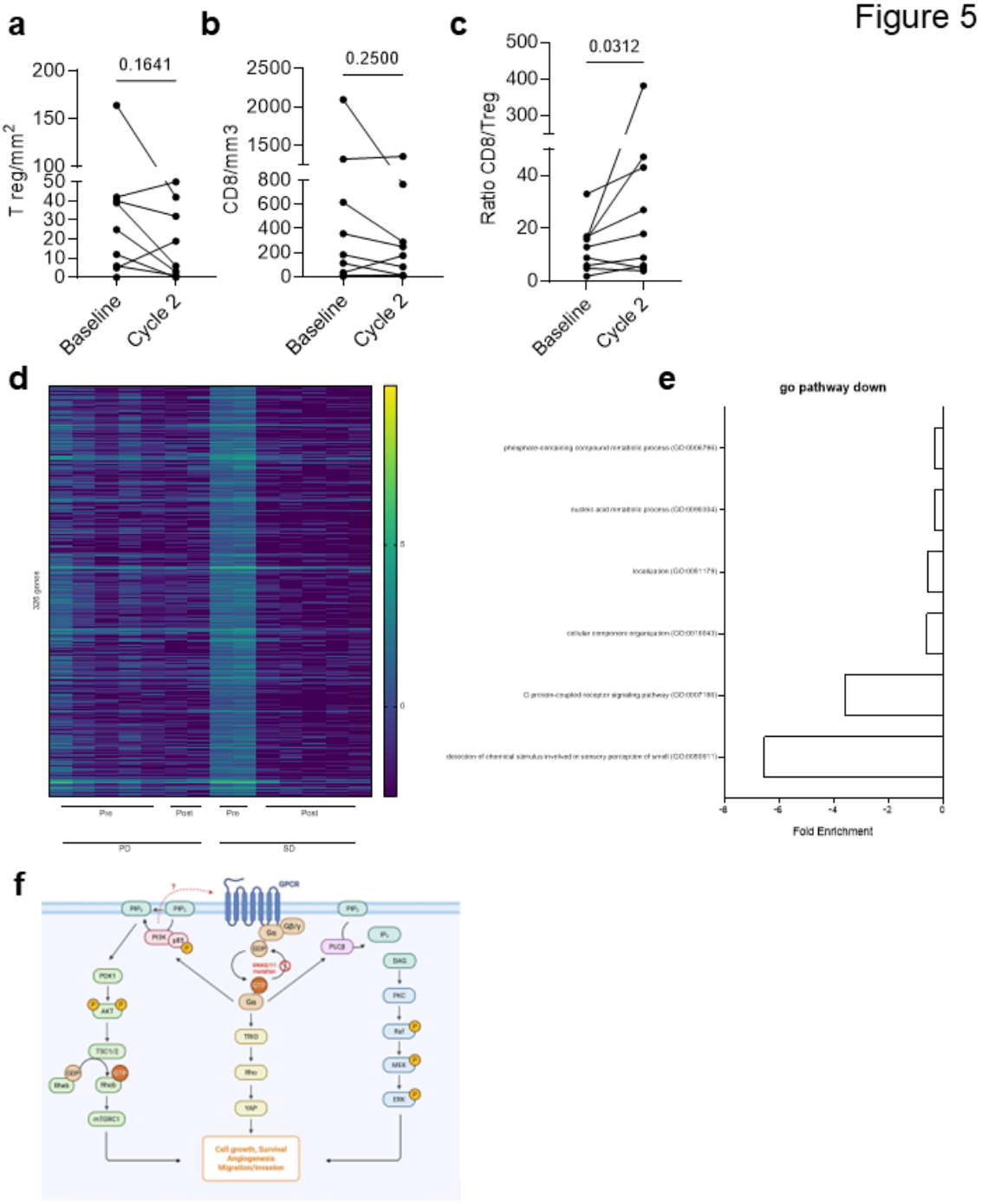


Figure 5

a-c Number of $CD8^+$ T cells and Tregs per mm^2 at Cycle 2 (i.e., 5 weeks after roginolisib treatment) compared to baseline measured by immunohistochemistry (IHC) in tumour tissue. **d** Heatmap of genes significantly downregulated in patients with SD at Week 16 after roginolisib treatment (17 tissue samples from 14 patients). **e** Gene Ontology pathway analysis found genes downregulated in patients with SD at Week 16. Patient-specific correlations were estimated and incorporated into the GO model.

Contrasts were then defined to compare conditions across treatment stages. **f** Graphical representation of the GPCR and PI3K signalling.

Supplementary Files

This is a list of supplementary files associated with this preprint. Click to download.

- DiGiacomoRogiFiHDoseStudySupplementaryFigures.pptx
- DiGiacomoRogiFiHDoseStudySupplementaryTables.docx
- DiGiacomoRogiFiHDoseStudySupplementaryFigLegends.docx